EUROPEAN UNION

Structural Instruments
2014-2020

Project co-financed by the European Regional Development Fund through the Competitiveness Operational Programme
“Investing in Sustainable Development”

Extreme Light Infrastructure-Nuclear Physics
(ELI-NP) - Phase II

Ion acceleration via ultra-intense laser

D. Doria
on behalf of RA3

Extreme Light Infrastructure (ELI-NP), Str. Reactorului no.30, P.O. box MG-6,
Bucharest - Magurele, Romania

domenico.doria@eli-np.ro

CAS18 – 27 Sep 2018, Constanta, Romania

Outline

Ion acceleration via ultra-intense laser

Laser matter interaction

Acceleration Mechanisms

Some laser ion acceleration history

Issues affecting the acceleration

Scaling Laws

What ELI can do

Laser matter interaction

Direct Laser Acceleration (DLA)

In 1957, Veksler envisioned the possibility of ‘coherent acceleration’:
a mechanism in which the accelerating field on each particle is proportional to the number of particle being accelerated, in contrast with conventional techniques.

V. Veksler, At. Energ. **2**, 525, (1957)

Veksler envisioned acceleration

$$\langle E \rangle \propto Nq \Rightarrow F \propto Nq^2$$

⬅ **Laser**

Conventional acceleration technique

$$\langle E \rangle \propto 1 \Rightarrow F \propto q$$

⬅ **Accelerator**

Direct Laser Acceleration (DLA)

Lawson-Woodward Theorem (J.D. Lawson, IEEE Trans. Nucl. Sci**. NS-26**, 4217, 1979)
the net energy gain of an electron interacting with an electromagnetic field in vacuum is zero.
Theorem axioms:

I. the laser field is in vacuum with no walls or boundaries present,
II. no static electric or magnetic field are present,
III. The region of interaction is infinite,
IV. Ponderomotive effects (non-linear forces, e.g. v x B force) are neglect.

Electromagnetic wave

$$E_k = E_0 e^{i(kx-\omega t)}$$

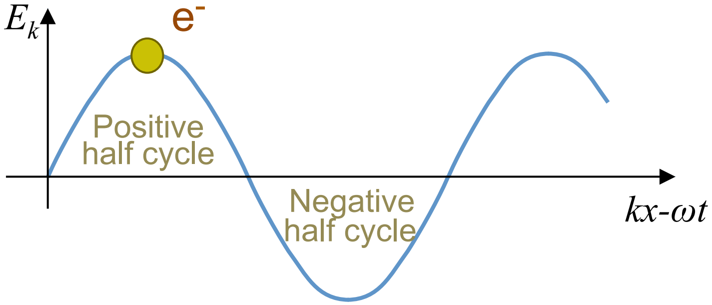

Average kinetic energy in one cycle

$$\langle W \rangle = \frac{1}{\tau}\int_0^{\tau} F \cdot v \; dt > 0$$

Average momentum in one cycle

$$\langle P \rangle = \frac{1}{\tau}\int_0^{\tau} F \; dt = 0$$

…No net work is done!
(*neglecting B, i.e. low laser intensity*)

Direct Laser Acceleration (DLA)

Lawson-Woodward Theorem (J.D. Lawson, IEEE Trans. Nucl. Sci. **NS-26**, 4217, 1979)

the net energy gain of an electron interacting with an electromagnetic field in vacuum is zero.

Theorem axioms:

I. the laser field is in vacuum with no walls or boundaries present,
II. no **static electric or magnetic field are present,**
III. The region of interaction is infinite,
IV. Ponderomotive effects (non-linear forces, e.g. v x B force) are neglect.

Conventional accelerators

Electromagnetic wave

$$E_k = E_0 e^{i(kx-\omega t)}$$

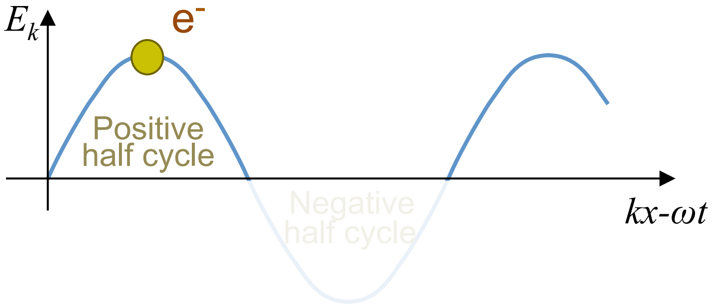

Average kinetic energy in one cycle

$$\langle W \rangle = \frac{1}{\tau}\int_0^\tau F \cdot v \, dt > 0$$

Average momentum in one cycle

$$\langle P \rangle = \frac{1}{\tau}\int_0^\tau F \, dt \neq 0$$

Static Accelerators

Paschen's law gives the breakdown voltage

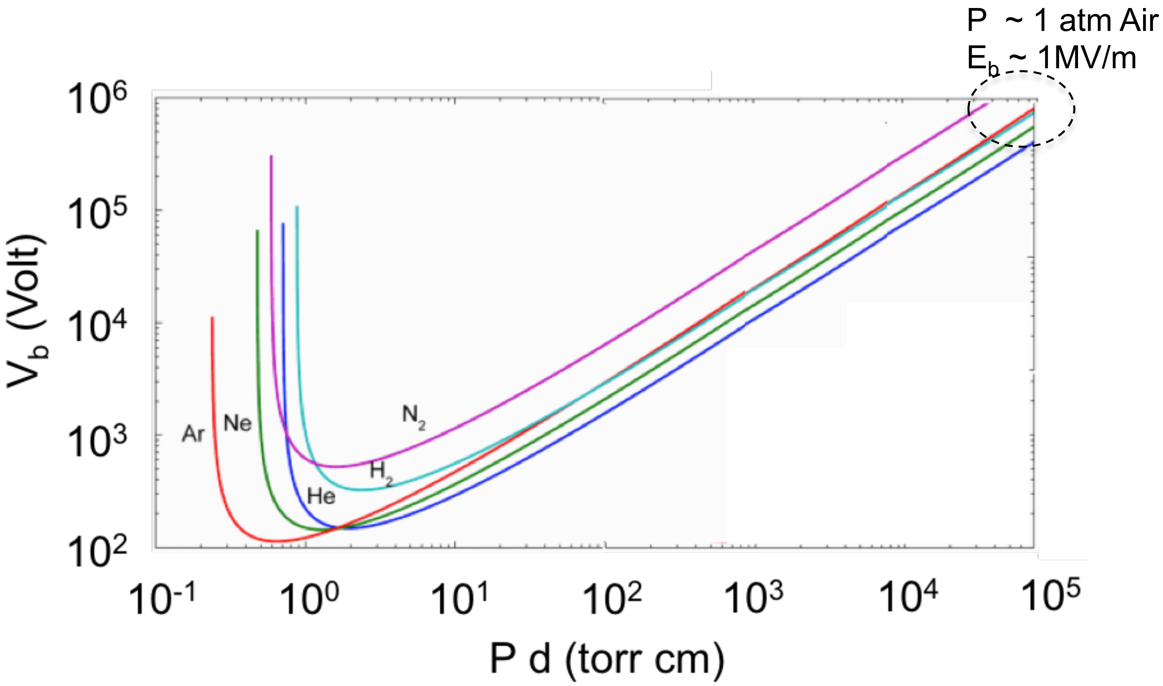

Tandem Van de Graaff

Brookhaven National Laboratory.

Breakdown Voltage

GAS

P ~ 1 atm Air E_b ~ 1 MV/m

P ~ 5 atm SF_6 E_b ~ 10s MV/m

SOLID

Porcelain E_b ~ 5 MV/m

Glass E_b ~ 100 MV/m

Max particle energy

e x E-field x distance = Energy

e x few MV/m x few m = 10 MeV

RF Accelerators

RF Cavity

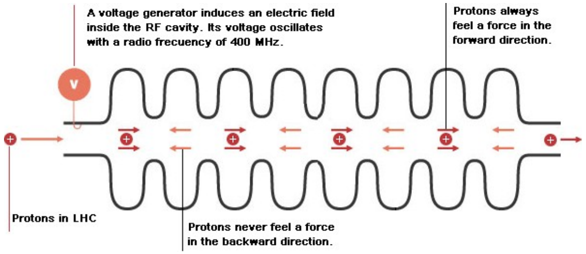

LINEAR ACCELERATOR RF

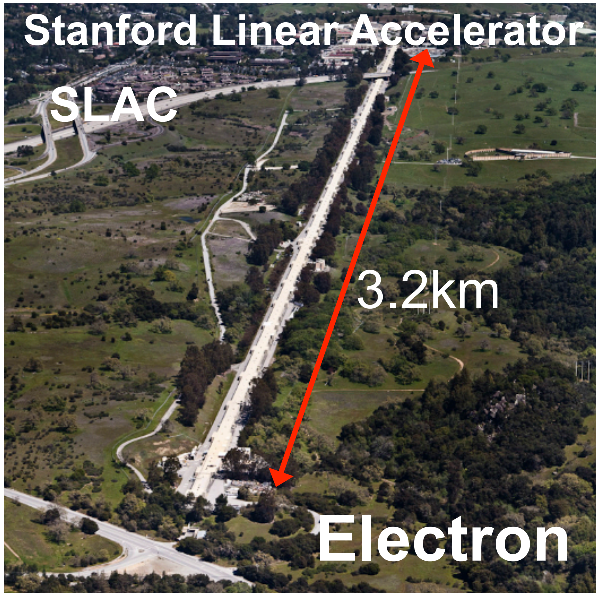

CIRCULAR ACCELERATOR RF

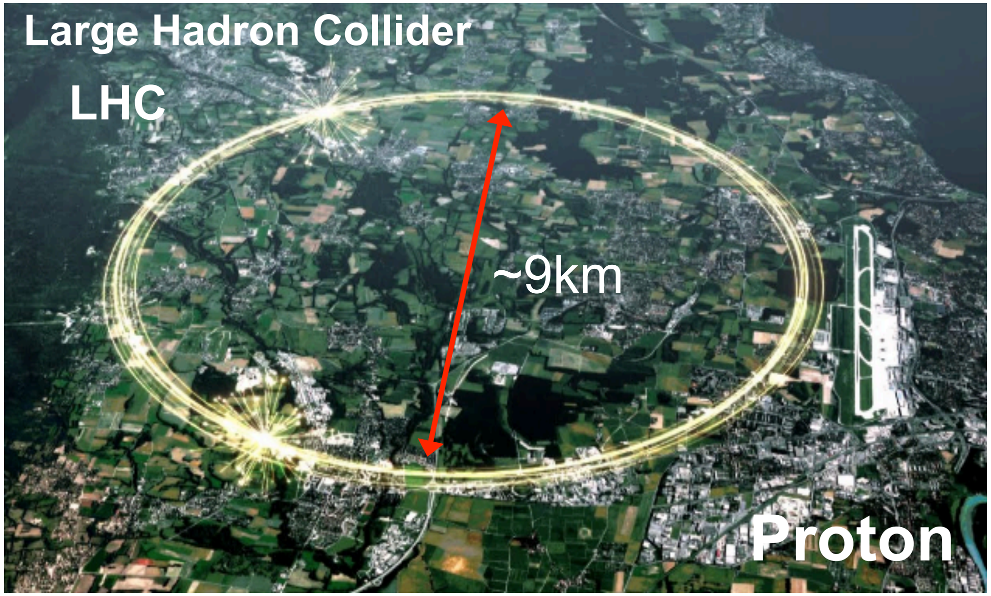

RF Cavities of 0.8MV 0

Take 10s μs to ~ 50 GeV electrons

Accelerating field 21 MV/m

8 RF Cavities of 2MV = 16 MeV/lap

11245 laps per second = 0.18 TeV/s

Take 10s of seconds to get to ~ 7 TeV protons

Accelerating field 5 MV/m

RF Accelerators

RF Cavity

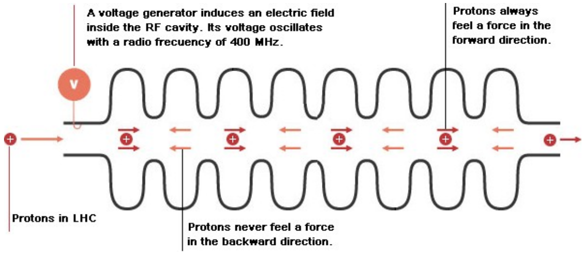

Laser ion acceleration

E-field > TV/m

10^6 times higher !

LINEAR ACCELERATOR RF

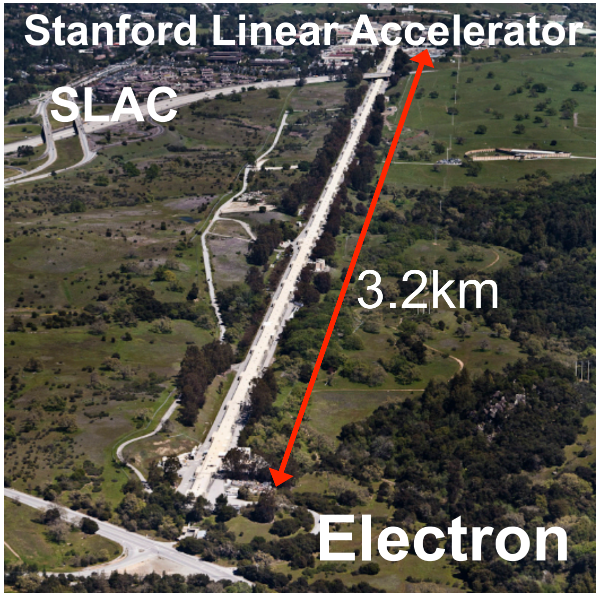

RF Cavities of 0.8MV 0

Take 10s µs to ~ 50 GeV electrons

Accelerating field 21 MV/m

CIRCULAR ACCELERATOR RF

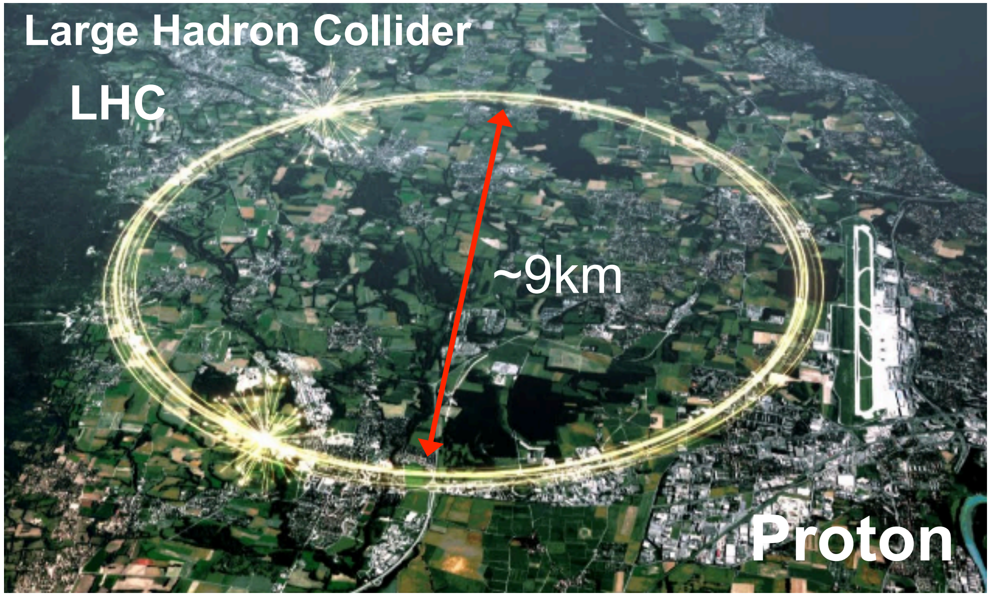

8 RF Cavities of 2MV = 16 MeV/lap

11245 laps per second = 0.18 TeV/s

Take 10s of seconds to get to ~ 7 TeV protons

Accelerating field 5 MV/m

Direct Laser Acceleration (DLA)

Lawson-Woodward Theorem (J.D. Lawson, IEEE Trans. Nucl. Sci**. NS-26**, 4217, 1979)

the net energy gain of an electron interacting with an electromagnetic field in vacuum is zero.

Theorem axioms:

I. the laser field is in vacuum with no walls or **boundaries present**,
II. no static electric or magnetic field are present,
III. The region of interaction is infinite,
IV. Ponderomotive effects (non-linear forces, e.g. v x B force) are neglect.

Electromagnetic wave packet

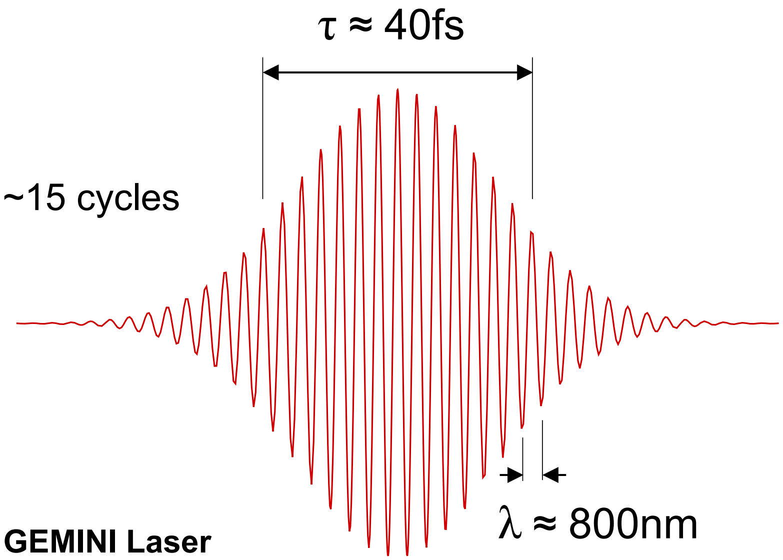

400TW GEMINI Laser
CLF - Rutherford Appleton Laboratory

Superposition of plane waves

$$E[x,t] = \frac{1}{\sqrt{2\pi}} \int_{-\infty}^{+\infty} E_k e^{i(kx-\omega[k]t)}\, dk$$

$$\omega^2 = c^2 k^2$$ dispersion relation in vacuum

Average kinetic energy in one cycle

$$\langle W \rangle = \frac{1}{\tau} \int_0^{\tau} F \cdot v\, dt > 0$$

Average momentum in one cycle

$$\langle P \rangle = \frac{1}{\tau} \int_0^{\tau} F\, dt \neq 0$$

Direct Laser Acceleration (DLA)

In 1957, Veksler envisioned the possibility of ‘coherent acceleration’: *a mechanism in which the accelerating field on each particle is proportional to the number of particle being accelerated, in contrast with conventional techniques.*

V. Veksler, At. Energ. **2**, 525, (1957)

How?

Boundaries (Plasma)

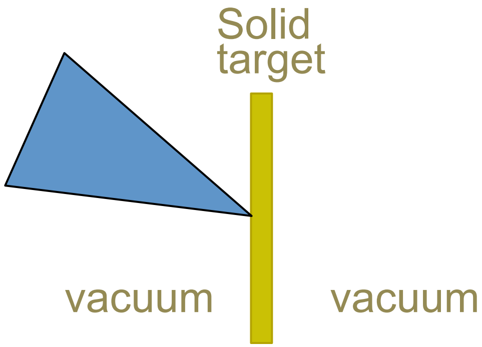

- Inverse Bremstrahlung
- Resonance absorption
- Vacuum Heating (or Brunel heating)

Non-linear effects

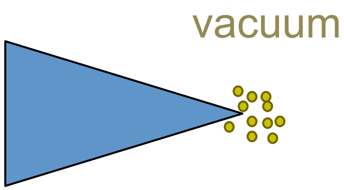

- Ponderomotive Force
- JxB Heating

Laser matter interaction

Boundaries (Plasma)

- Inverse Bremstrahlung
- Resonance absorption
- Vacuum Heating (or Brunel heating)

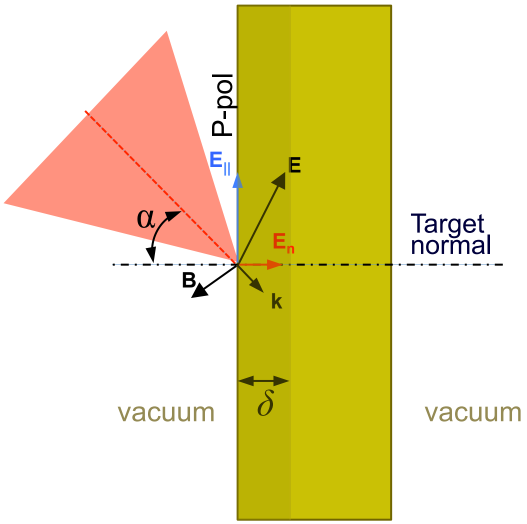

- Electrons are pushed beyond the skin depth in less than half laser cycle via direct acceleration or via plasma oscillation modes
- They acquires a velocity of the order of the quiver velocity:
  - Low velocity ➔ collisional motion (e.g. inverse Bremstrahlung)
  - High velocity ➔ collisionless motion (e.g. Resonance absorption)
- They generate a charge displacement that create an electric field
- The electric field accelerates ions

$$v_{quiver} = \frac{eE_0}{m_e\omega} \Rightarrow \frac{\overbrace{eE_0 c/\omega}^{\text{Electron Kinetic energy}}}{\underbrace{m_e c^2}_{\text{Electron rest energy}}} \overset{def}{=} a_0$$

Dispersion relation of a Light wave in Plasma

$$\boxed{\omega^2 = \omega_{pe}^2 + c^2k^2 > \omega_{pe}^2} \quad ,\forall k \in \Re$$

$$\omega_{pe} = \sqrt{\frac{4\pi n_e e^2}{m_e}} \quad , \quad \omega_{pe} \sim 10^{16} \text{ rad/s}$$

for solid target

Refractive index $n \cong \sqrt{1 - \frac{\omega_{pe}^2}{\omega^2}}$

$\omega > \omega_{pe}$ can penetrate inside

$\omega < \omega_{pe}$ is dumped at the interface

$$\delta = \frac{c}{\sqrt{\omega_{pe}^2 - \omega^2}} \cong \frac{c}{\omega_{pe}}$$

skin depth

Critical density $n_c = \frac{m_e \omega_L^2}{4\pi e^2} \quad ,(\omega_{pe} \to \omega_L)$

$\lambda_{LASER} \approx 1\mu m$

Typical solid target density, n_e

➔

$n_e \sim 10s\ n_c$

$\delta \sim 10s$ nm

$\delta/c < 1s$ fs

Laser matter interaction

Non-linear effects

- Ponderomotive Force
- JxB Heating

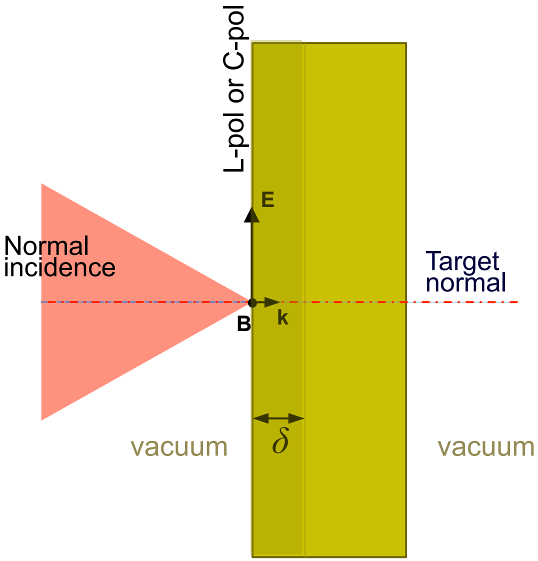

Ponderomotive Force

It is generated by spatial gradients in the intensity of the electromagnetic wave and it corresponds to the more general concept of light pressure

Non-relativistic
Ponderomotive force

$$F_p = -\frac{\omega_{pe}^2}{\omega^2}\frac{\nabla\langle E^2\rangle}{8\pi}$$

Relativistic
Ponderomotive force

$$F_p = -m_e c^2 \nabla(\gamma - 1)$$

$$F_p \overset{def}{=} -\nabla U_p$$

Non-relativistic
Ponderomotive potential

$$U_p = \frac{\omega_{pe}^2}{8\pi\,\omega^2}\langle E^2\rangle$$

Relativistic
Ponderomotive potential

$$U_p = m_e c^2 (\gamma - 1)$$

$$\gamma = \sqrt{1 + a_0 / 2}$$

JxB Heating

At high laser intensity (i.e. relativistic motion of electrons), **JxB** component of the Lorentz force becomes comparable with the transverse motion associated with the electric field and generates a significant longitudinal push.

Drift velocity of an electron

Lorentz Force

$$\frac{dp}{dt} = -e\left(E + \frac{v}{c}\times B\right)$$

$$J \propto ev \;\Rightarrow\; J \parallel v \;\;(\sim\; \parallel E)$$

$$J \times B \sim \boxed{E \times B \;\parallel\; k}$$

Drift velocity direction

Laser matter interaction

Light pressure

Equations of motion of a free electron interacting with a monochromatic plane wave

$A(kx-\omega t)$ with amplitude A_0 and $E=-\frac{1}{c}\partial_t A$, $B=\nabla\times A$

Dimensionless amplitude

$$a_0=\frac{eE_0}{m_e c\,\omega}=\frac{eA_0}{m_e c^2}\qquad \frac{\text{Electron Kinetic energy}}{\text{Electron rest energy}}$$

$$a_0=\sqrt{\frac{E_0^2\lambda^2}{m_e^2c^4}}\sim\lambda\sqrt{I_0}$$

Linear polarization

$$\tau=t-x(t)/c$$

$$x(\tau)=\frac{ca_0^2}{4}\left[\tau+\frac{1}{2\omega}\sin(2\omega\tau)\right]$$

$$y(\tau)=\frac{ca_0}{\omega}\sin\omega\tau$$

self-emission

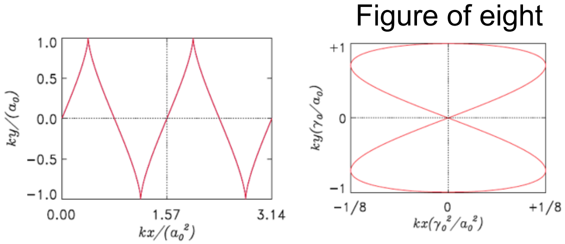
Figure of eight

Circular polarization

$$x(\tau)=\frac{ca_0^2\tau}{4}$$

$$y(\tau)=\frac{ca_0}{\sqrt{2}\omega}\sin(\omega t/\gamma)$$

$$z(\tau)=\mp\frac{ca_0}{\sqrt{2}\omega}\cos(\omega t/\gamma)$$

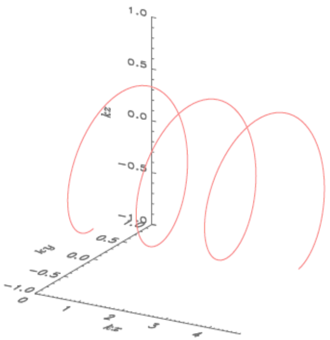

$$a_0=\rho\sqrt{\frac{I_0\lambda^2}{10^{18}Wcm^{-2}\mu m^2}}$$

$\rho=$ 0.85 Linear polarization

0.60 Circular polarization

0.5PW GEMINI Laser

CLF - Rutherford Appleton Laboratory

$\lambda\approx$ 800nm

$I_0\approx$ 10^{21} W/cm^2

$a_0\sim 25$

Drift velocity

$$v_d=\frac{a_0^2}{a_0^2+4}c$$

First experiments with Laser

The **first laser** was built in **1960** by Theodore H. Maiman at Hughes Research Laboratories, based on theoretical work by Charles Hard Townes and Arthur Leonard Schawlow

Laser acceleration of ions from laser irradiated targets was studied from 1960s throughout the 90s at laser Intensity below 10^{16} W/cm^2

Laser couples energy into electrons
Faster electrons drag ions
Self-similar model of free expanding plasma in vacuum

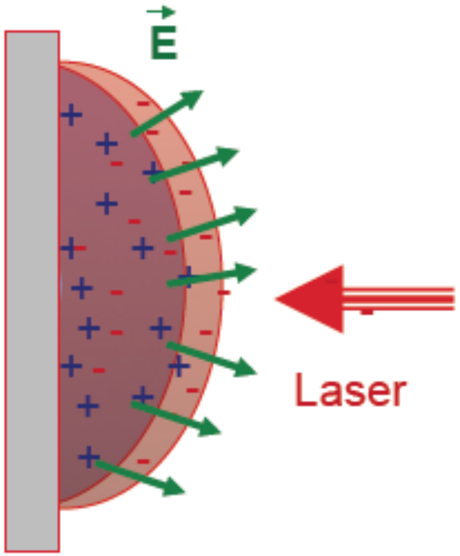

A.V. Gurevich et al, Sov. Phys. JETP, 22, 449 (1966)

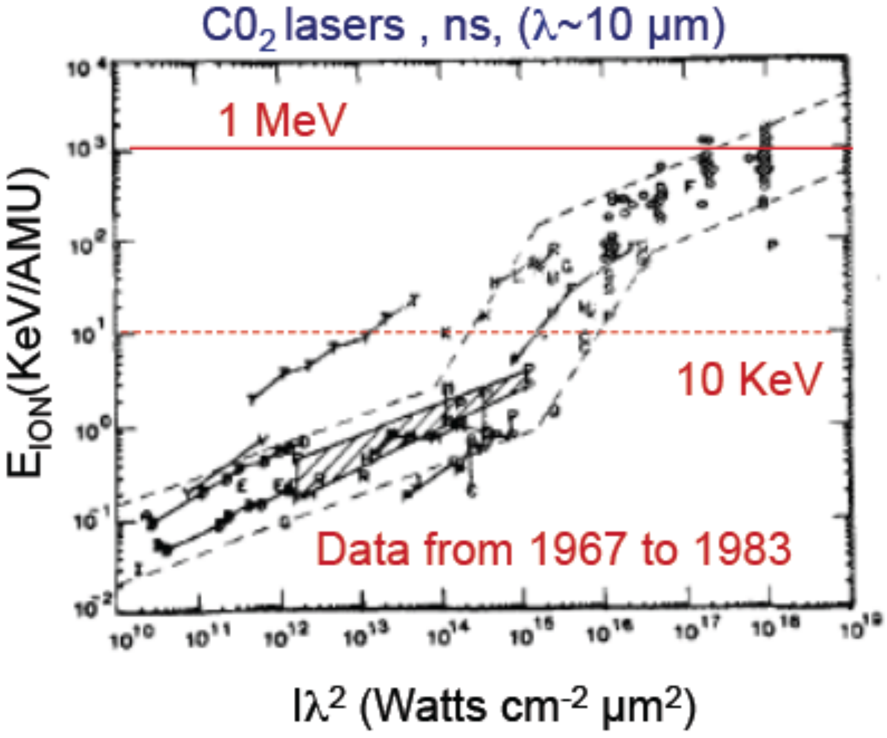

S.J. Gitomer et al, Phys. Plasmas, 29, 2679 (1986)

High Power Laser history

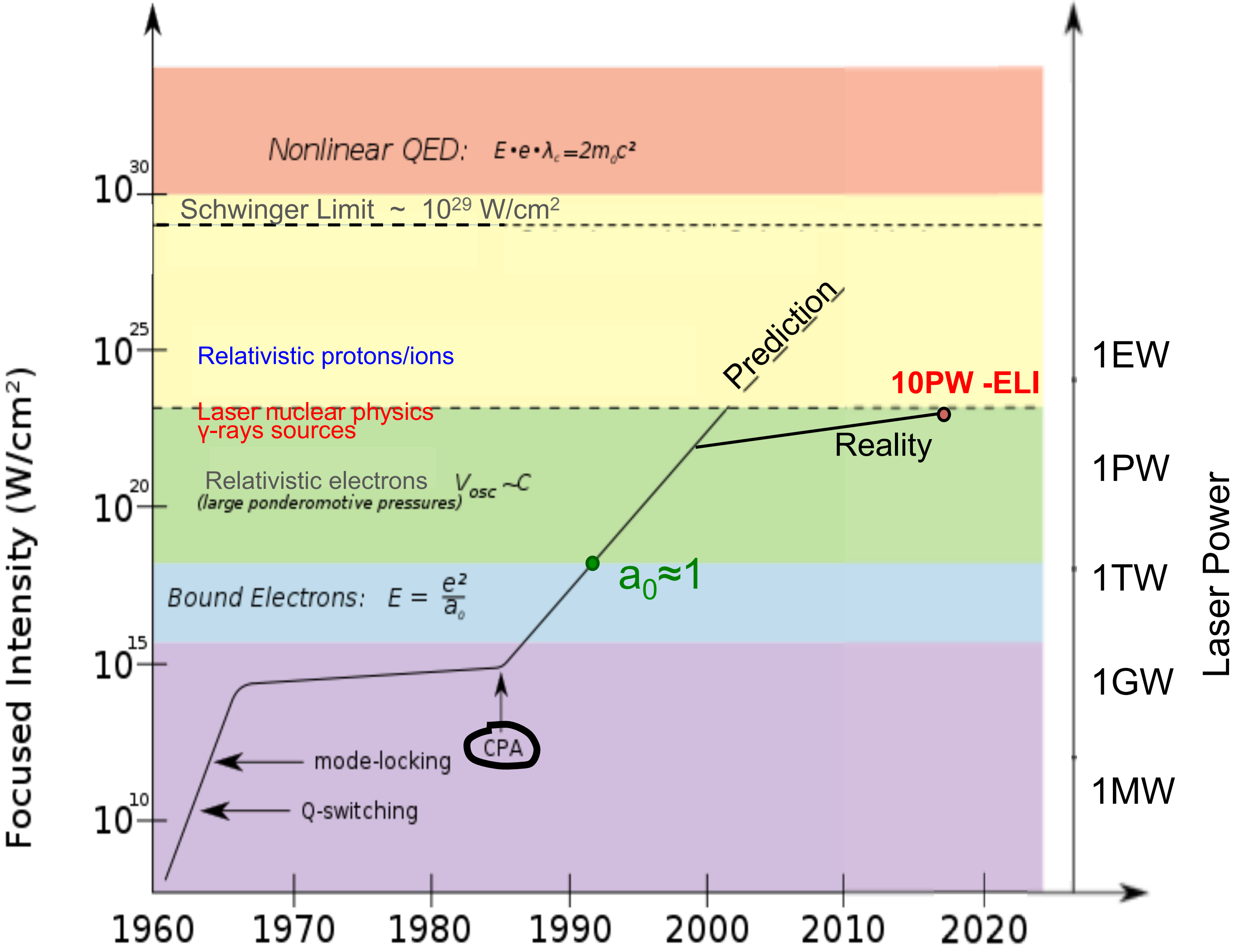

Chirped pulse amplification (CPA)

G. E. Cook,"Pulse Compression-Key to More Efficient Radar Transmission", IEEE Proc. IRE 48, 310 (1960)

D. Strickland and G. Mourou, “Compression of amplified chirped optical pulses”, Opt. Commun. 56, 219 (1985)

Typical Exp. setup

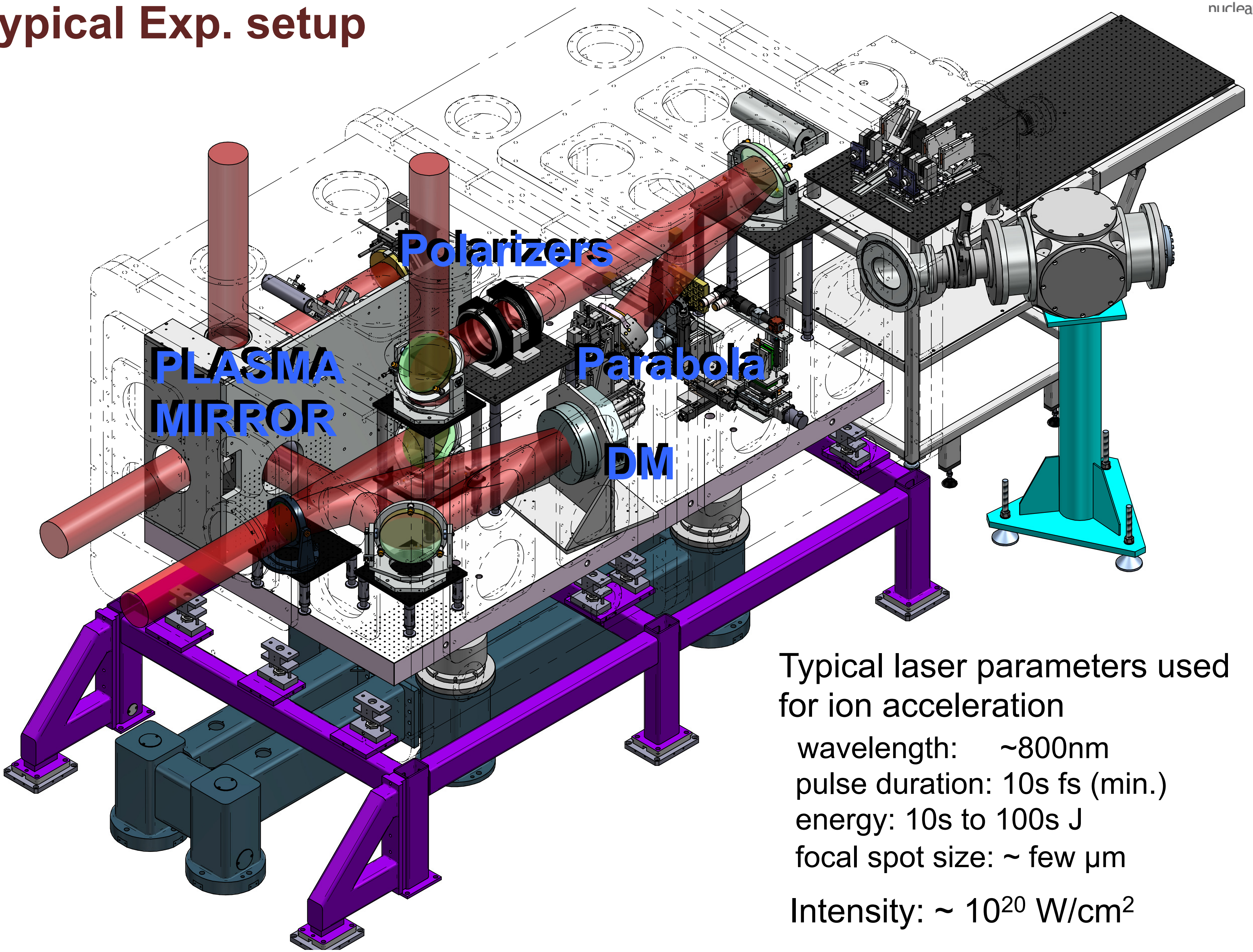

Typical laser parameters used for ion acceleration

wavelength: ~800nm
pulse duration: 10s fs (min.)
energy: 10s to 100s J
focal spot size: ~ few µm

Intensity: ~ 10^{20} W/cm^2

Acceleration mechanisms

Sheath (surface) acceleration:
(in micron-thick targets)

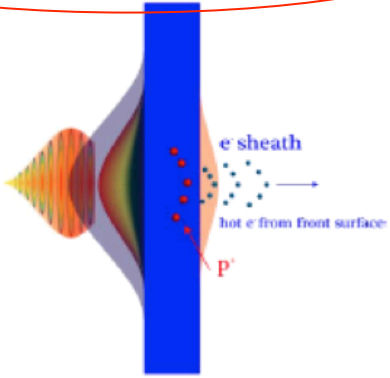

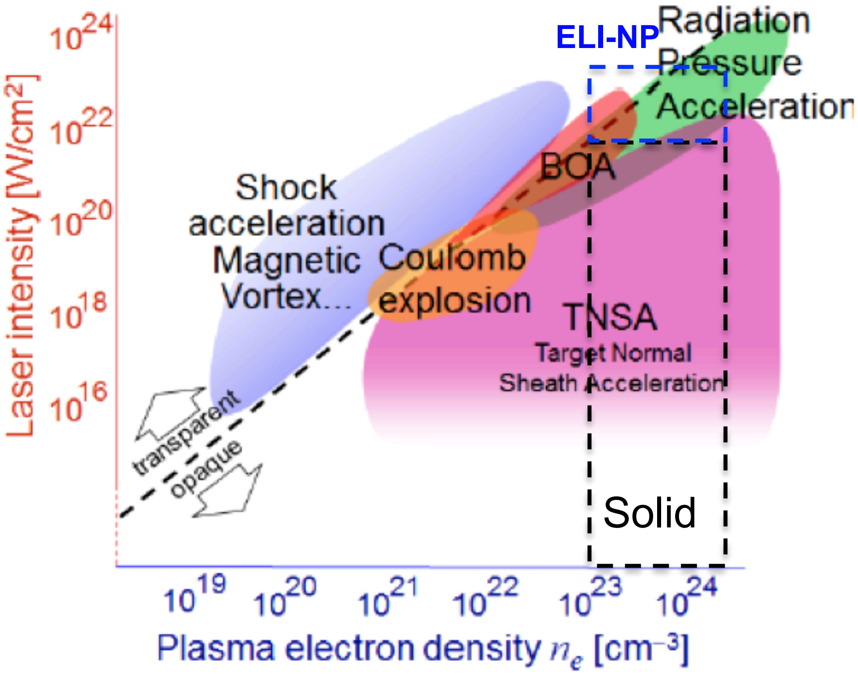

Volumetric acceleration:
(in nanometre-thick targets)

Radiation pressure acceleration

Hole-Boring

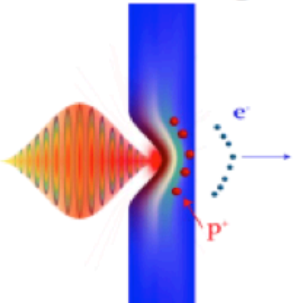

Light Sail

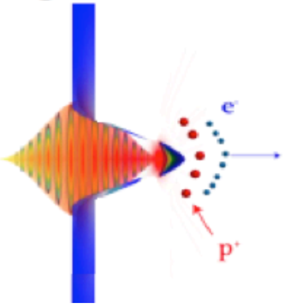

Relativistic transparency
(BOA) regime

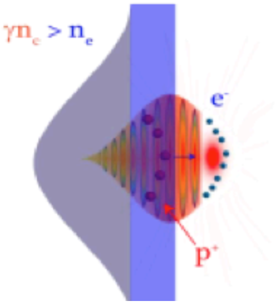

TNSA mechanism

Target Normal Sheath Acceleration (TNSA)

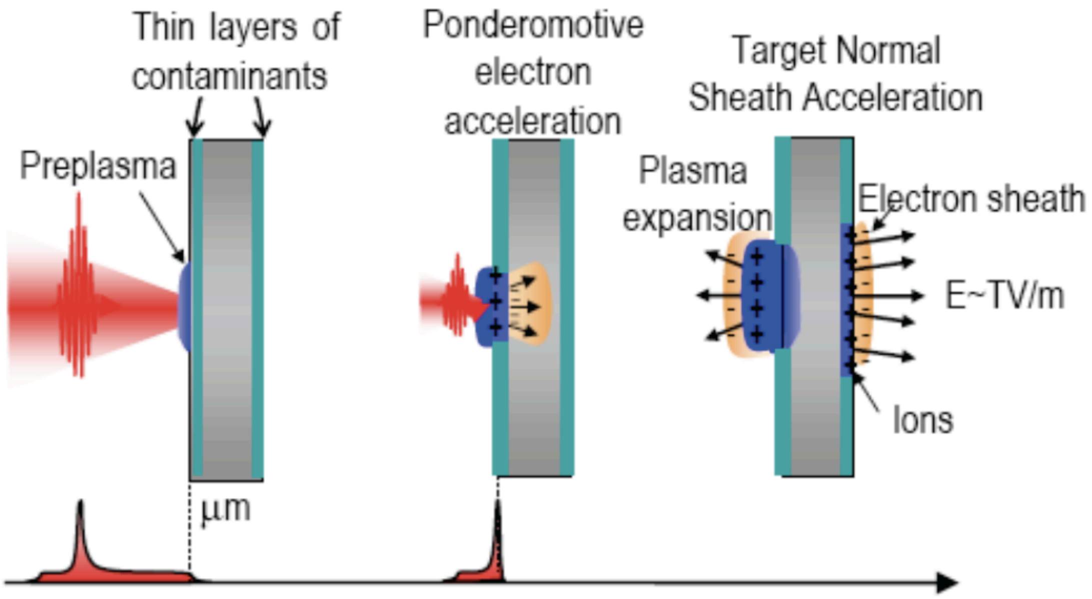

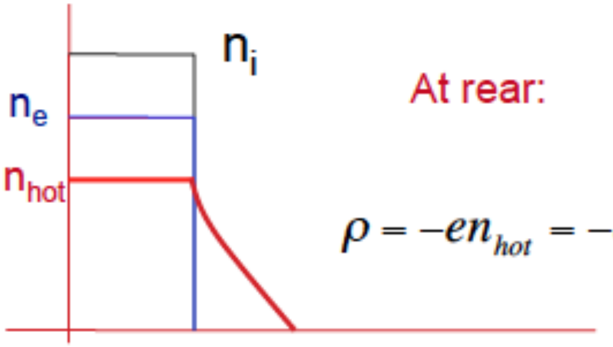

At rear:

$$\rho = -en_{hot} = -en_0 \exp\left(-\frac{x}{\lambda_D}\right)$$

Energy balance

Ponderomotive push

$$kT_{hot} \approx U_p = m_e c^2 \left(\sqrt{1 + \frac{a_0}{2}} - 1\right)$$

Linear polarization

$$a_0 = \sqrt{\frac{I_0 \lambda^2}{1.38x10^{18}\,Wcm^{-2}\mu m^2}}$$

Acceleration Field

$$eE_s \lambda_D \approx kT_{hot}$$

$$E_s \approx \frac{kT_{hot}/e}{\delta} \sim \frac{\sim MV}{\sim um} = 10^{12}\ V/m$$

S.P.Hatchett *et al*, Phys Plasmas, **7**, 2076 (2000)
P.Mora et al, PRL, **90**, 185002 (2003)

TNSA mechanism

Target Normal Sheath Acceleration (TNSA)

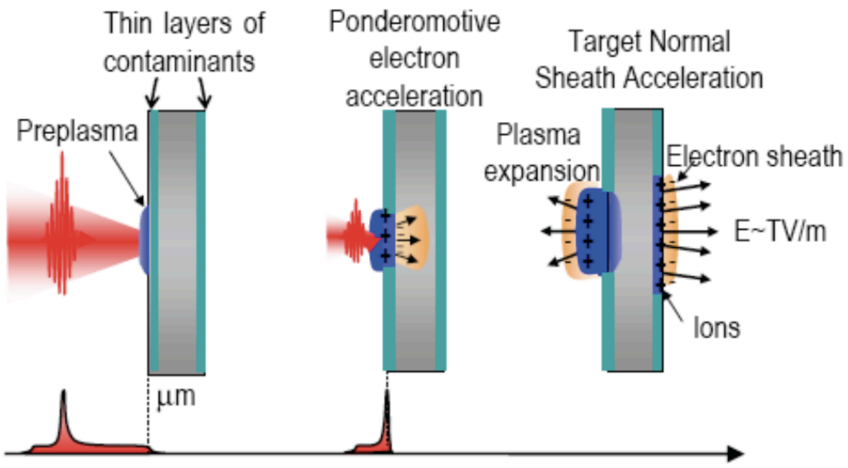

TNSA Proto spectrum

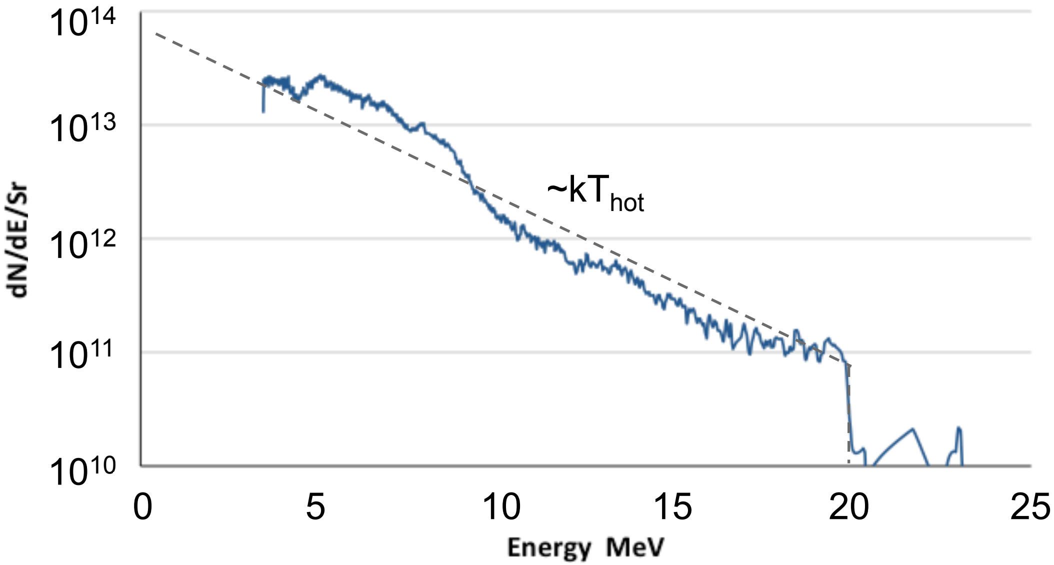

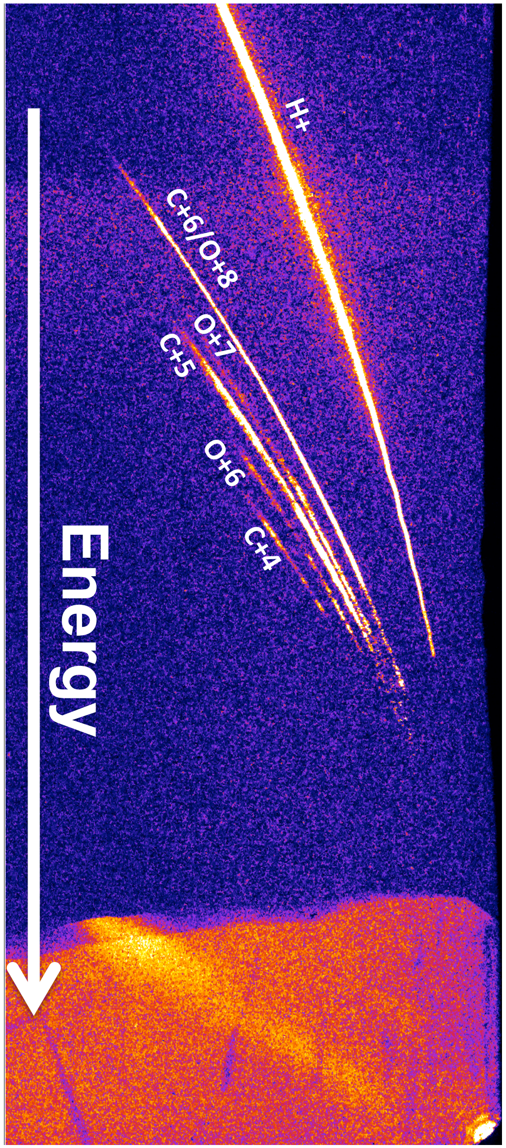

TNSA characteristics

Target Normal Sheath Acceleration (TNSA) Characteristics

- Broad spectrum (LHC monoenergetic)
- short pulse duration (< 100s ps)
- diverging beams (10s of deg) (LHC collimated)

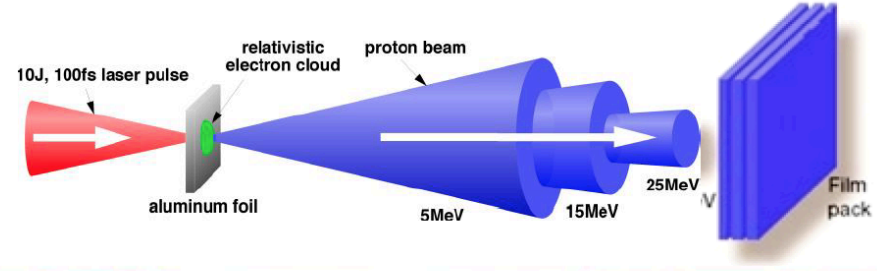

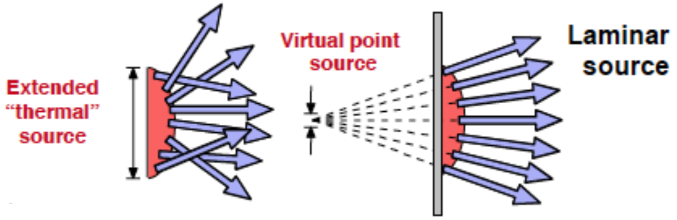

- Low emittance/ high laminarity

  0.1 π mm mrad @ >15 MeV (LHC protons ~ 1.7)

- High brightness

  $10^{11} – 10^{13}$ protons(ions) in a single shot (>3 MeV) (LHC ~ 10^{11} p/bunch)

- acceleration distance ~ 10s microns (LHC ~ km)
- Accelerating field ~ 10^{12} V/m (LHC ~ $5x10^{6}$ V/m)

Beginning of experiments with high-power lasers

R. Clark *et al.*, PRL 85, 1655 (2000)

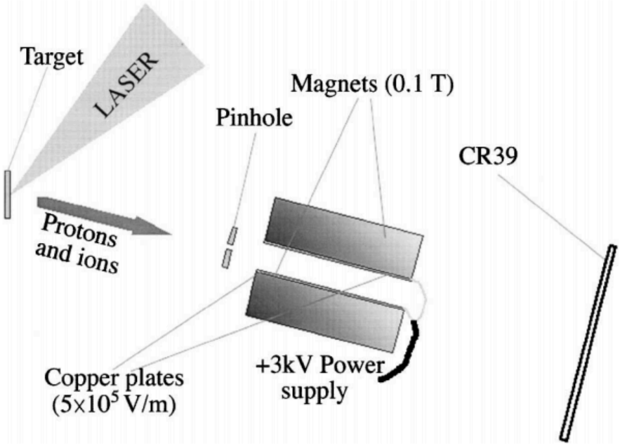

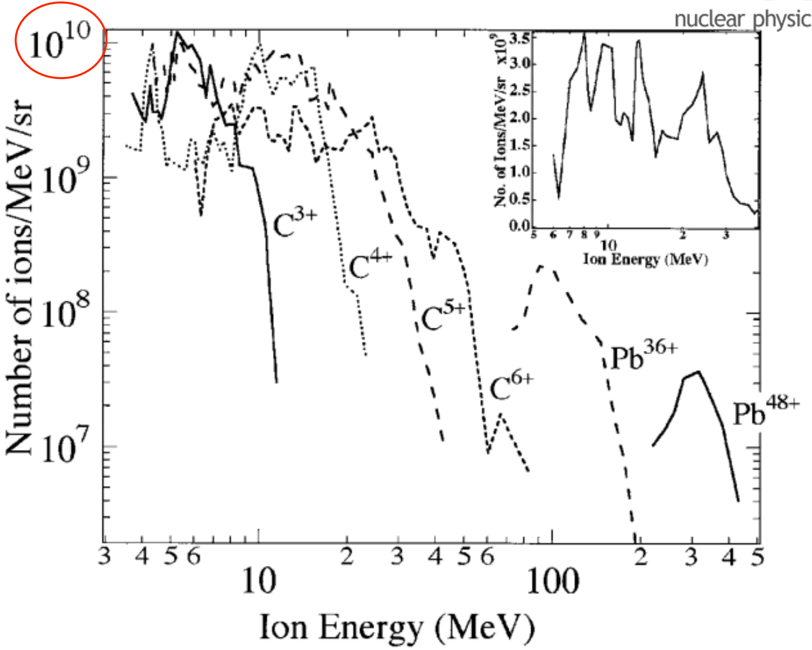

50TW CLF Vulcan System (2000yr)

t_L ~ 1ps
λ =1054nm

Laser spot (FWHM) of 10μm dia.
(p-polarization, at 45º)

Laser energy ~50 J,
Peak Intensity ~ 5x10^{19} W/cm^2

Pb target

- Most of the energy go onto the protons
- Max energy scales proportionally to the charge
- Cleaning from contaminants give more energy to bulk ion

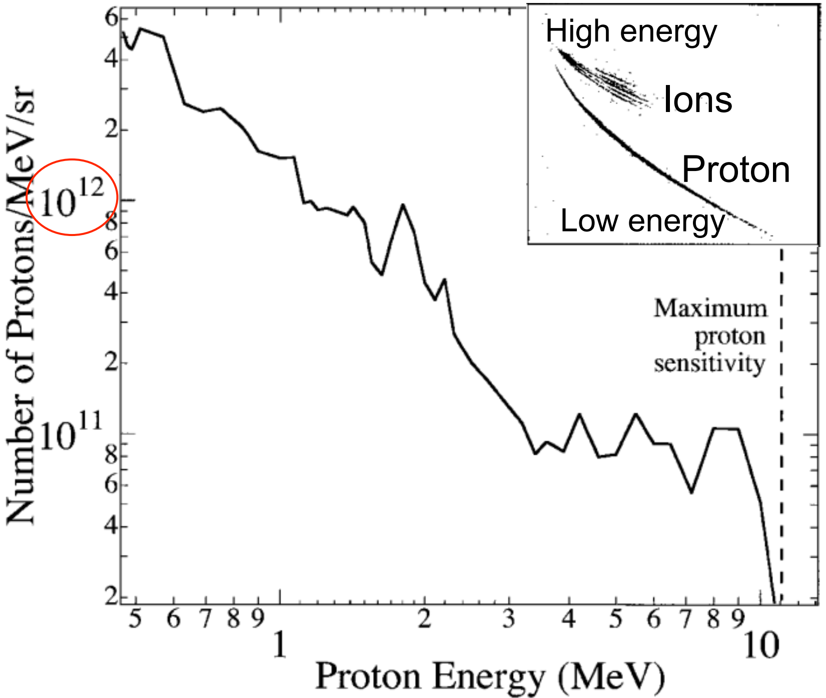

Varying target any ion can easily be accelerated
(not straightfoward with RF accelerators)

Beginning of experiments with high-power lasers

R. Clark *et al.*, PRL 85, 1655 (2000)

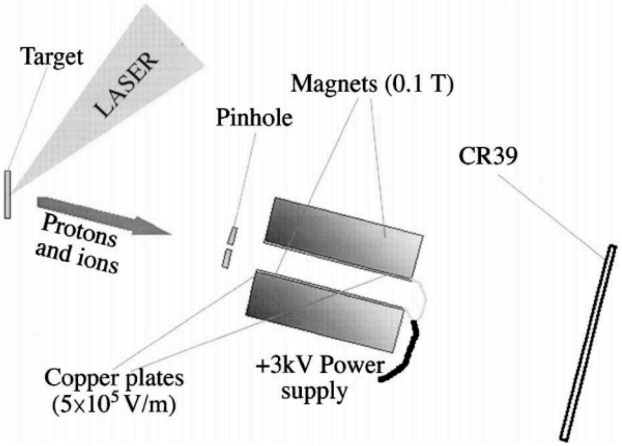

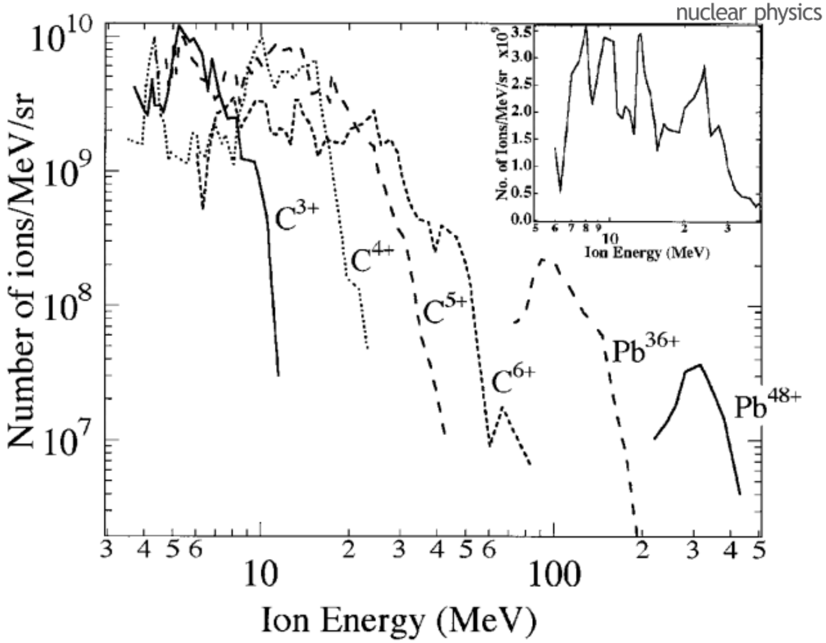

50TW CLF Vulcan System (2000yr)

t_L ~ 1ps
λ =1054nm

Laser spot (FWHM) of 10µm dia.
(p-polarization, at 45º)

Laser energy ~50 J,
Peak Intensity ~ 5×10^{19} W/cm^2

Pb target

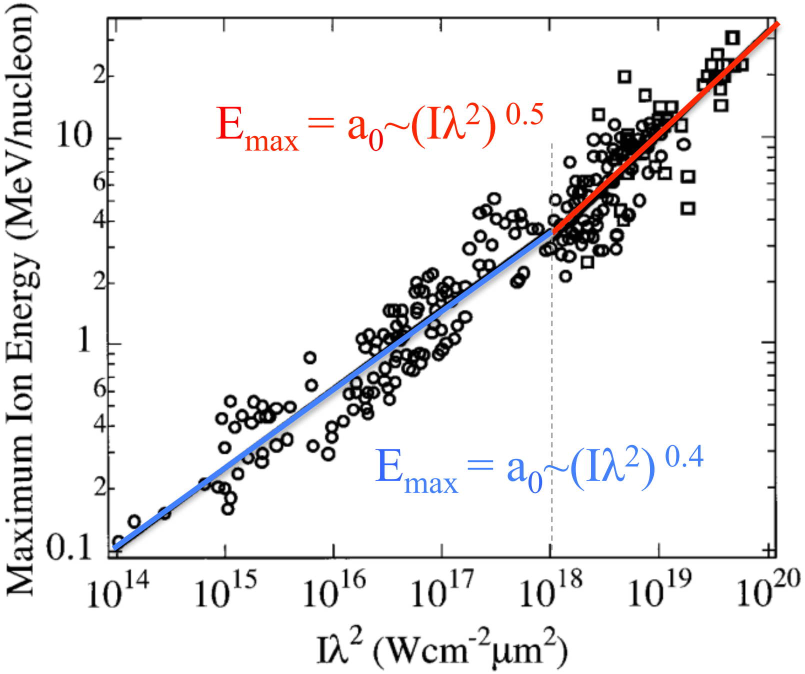

- Most of the energy go onto the protons
- Max energy scales proportionally to the charge
- Cleaning from contaminants give more energy to bulk ion

Varying target any ion can easily be accelerated
(not straightfoward with RF accelerators)

What do we want from TNSA?

Increasing particle energy

Increasing conversion efficiency

Narrowing the spectral band

Collimated beam

Shorten bunch size

How can we do it?

Reduction of foil thickness

Multi-pulse for shaping proton beam

Target structuring for enhanced coupling

Reduction of mass targets

Enhanced beam properties by post acceleration

Reduction of target thickness

D. Neely *et al.*, APL 89, 021501 (2006)

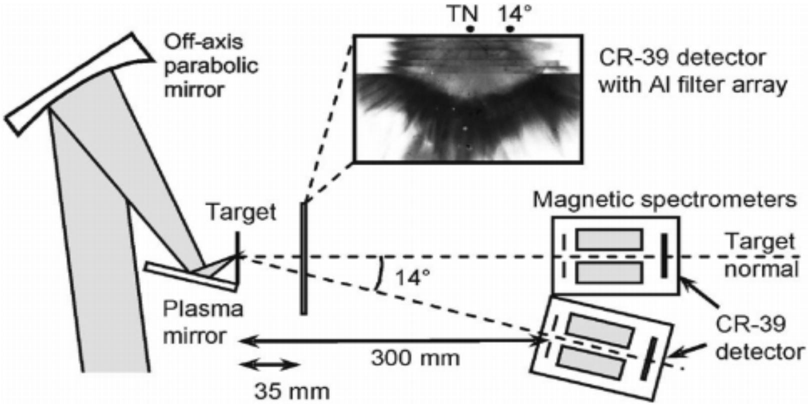

20TW Lund Laser Centre System

t_L ~ 33fs
λ =800nm

Laser spot (1/e^2) of 10µm dia.
(p-polarization, at 30º)

Laser energy ~0.7 J,
Laser energy after PM ~ 0.3 J (~40%)
Contrast ~ 10^8 ➔ ~ 10^{10}
Peak Intensity ~ 10^{19} W/cm^2

Thickness Al targets
from **30µm** down to **20nm**

If no PM is used the ASE will launch a shockwave with the speed of 8µm/ns. So that a rear surface of a target with thickness < few µm will be destroyed by the ASE before the main pulse arrives

Laser time profile

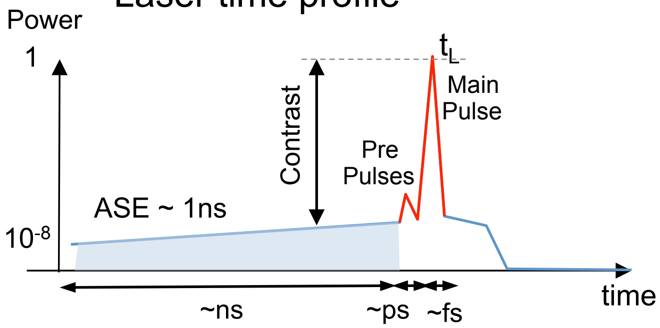

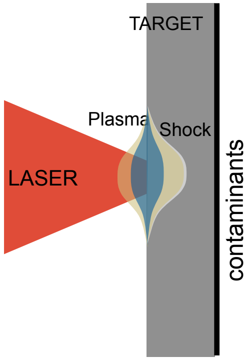

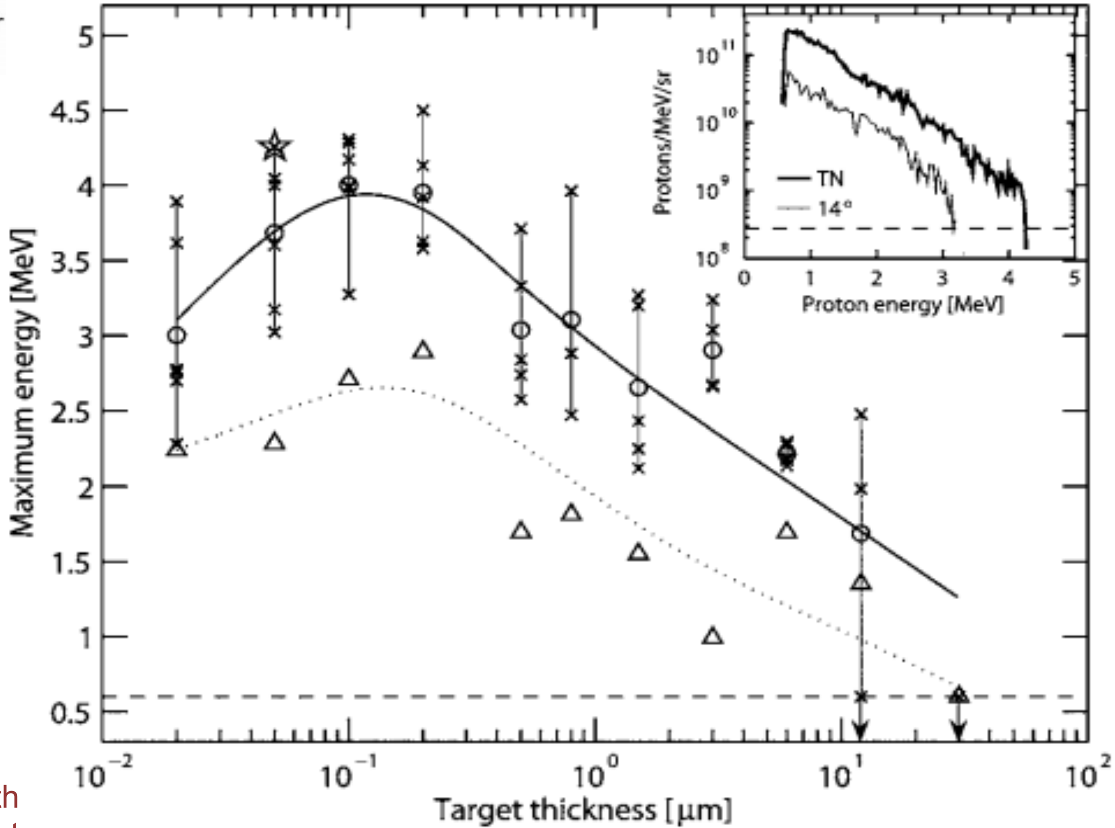

Maximum proton energies obtained as a function of Al target thickness for on-target contrasts of 10^{10} crosses. The solid line is a trend line fitted to the on-axis average for each thickness circles.

Multi-pulse for enhancing energy coupling

C. Brenner *et al.*, APL 104, 081123 (2014)

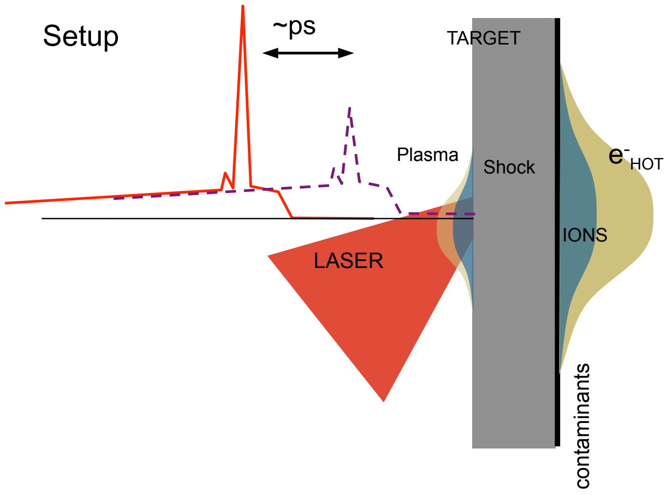

Laser time profile

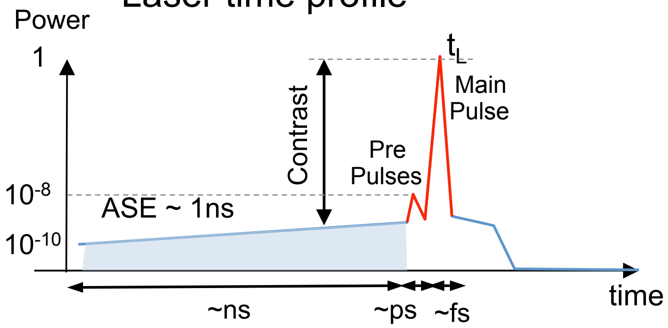

1PW CLF Vulcan System

t_L ~ 800fs
λ =1054nm

Laser spot (FWHM) of 30μm dia.
(p-polarization, at 45º)

Laser energy main ~180 J
Contrast ~ 10^{10} (ns) and ~ 10^{8} (ps)
Peak Intensity main ~ 2.9x10^{19} W/cm^2
Peak Intensity sec. ~ 3.2x10^{18} W/cm^2

Time delay btw pulses form 0 to 4ps

Au target 5μm thick

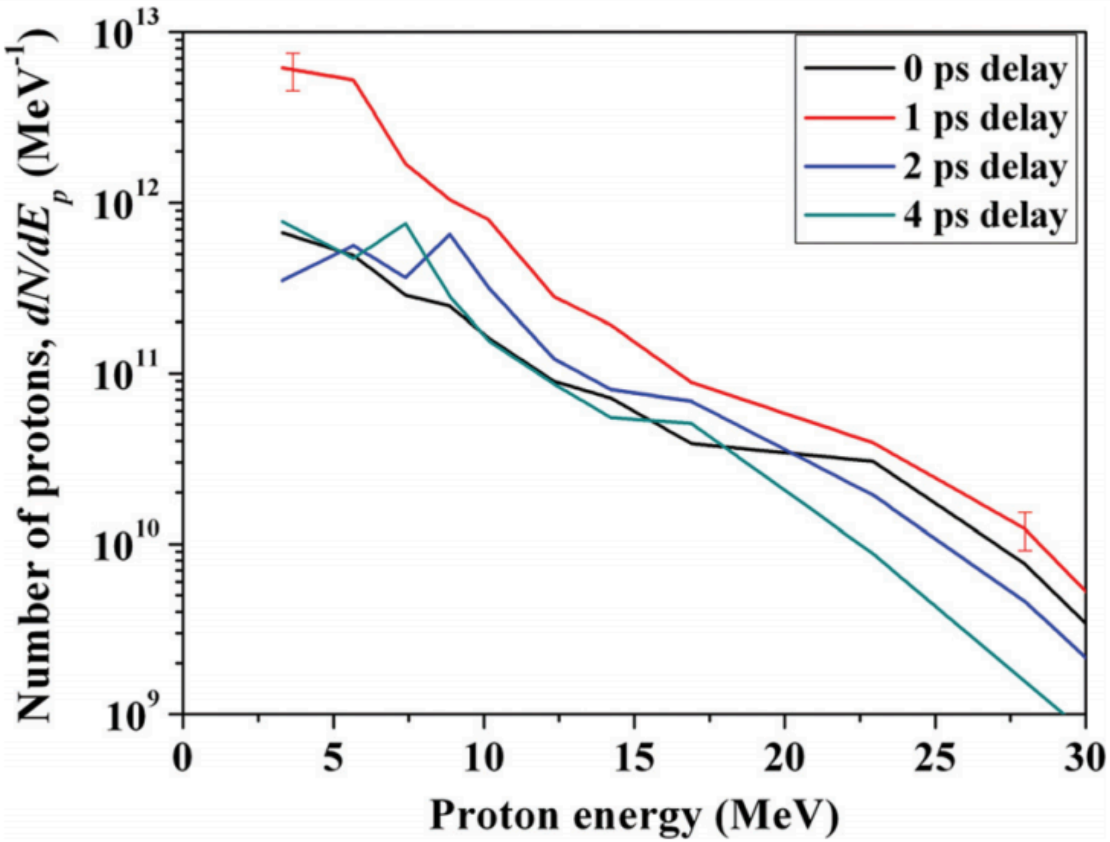

Proton energy spectra obtained from 5 μm-thick targets with single pulse (t_{delay} = 0 ps) and double-pulse (t_{delay} = 1, 2, and 4 ps) irradiation. Sample errorbars are shown for the 1 ps delay spectrum.

Multi-pulse for enhancing energy coupling

C. Brenner *et al.*, APL 104, 081123 (2014)

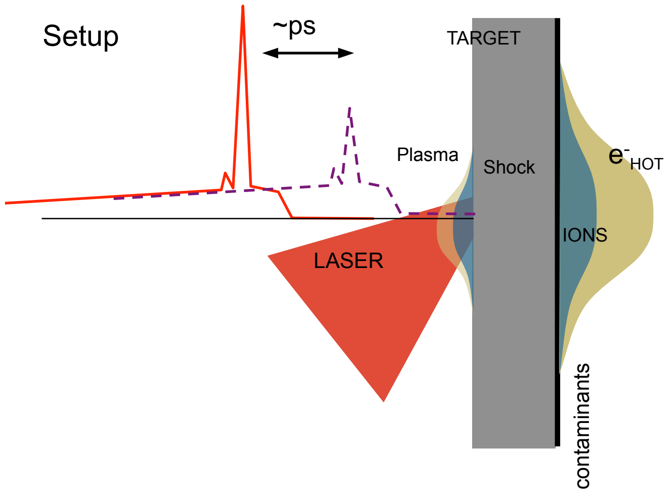

Laser time profile

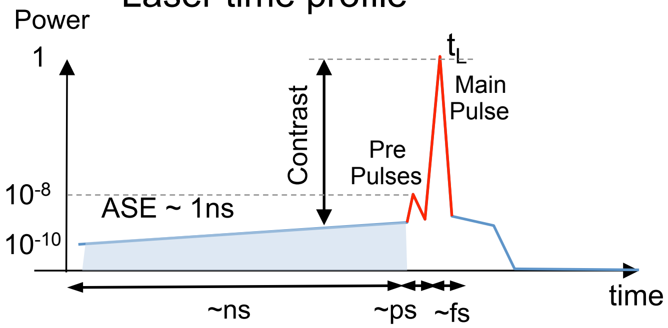

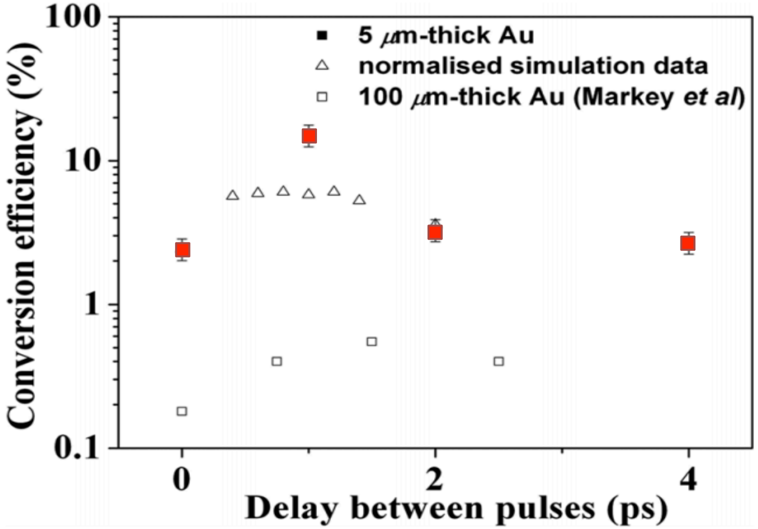

Laser-to-proton energy conversion efficiency with respect to t_{delay} obtained for 5 Im-thick Au targets compared to results obtained with thicker (100 Im-thick, Au targets. Simulated laser-to-proton energy conversion efficiency with respect to t_{delay} normalised to the single pulse measured value is also shown.

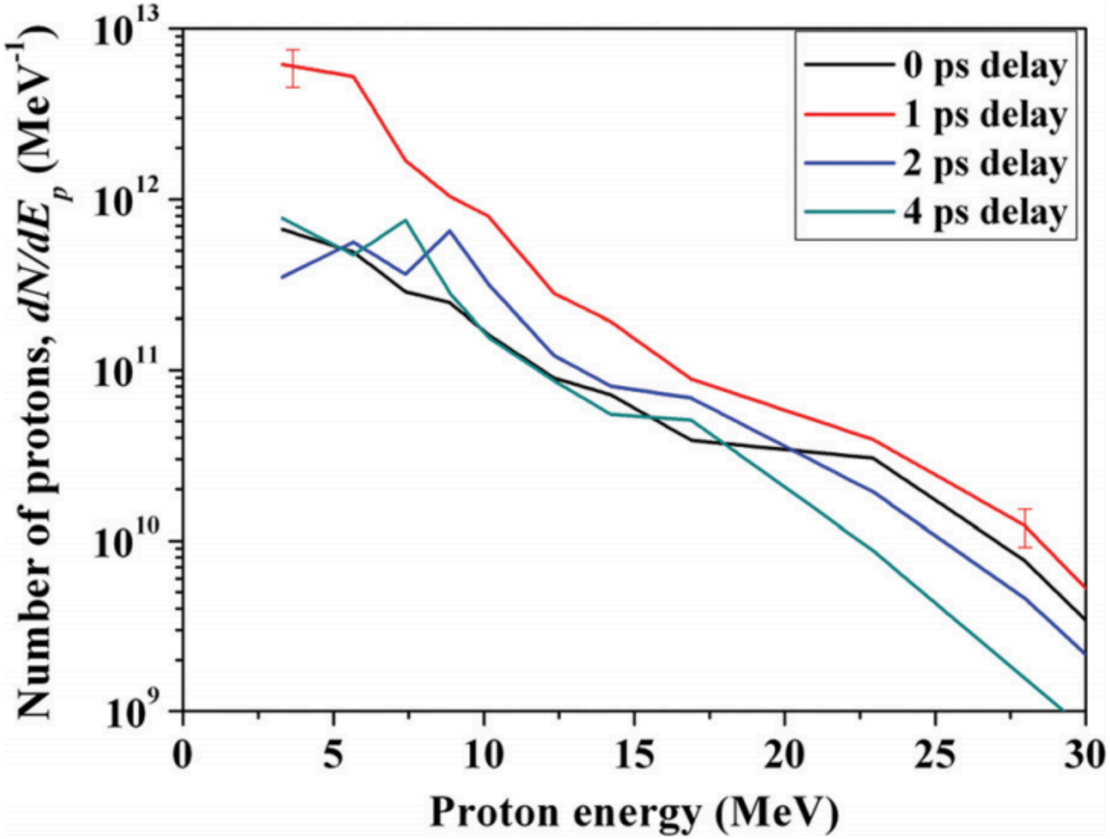

Proton energy spectra obtained from 5 μm-thick targets with single pulse (t_{delay} = 0 ps) and double-pulse (t_{delay} = 1, 2, and 4 ps) irradiation. Sample errorbars are shown for the 1 ps delay spectrum.

Target structuring for enhanced coupling

D. Margarone *et al.*, PRL 109, 482310 (2012)

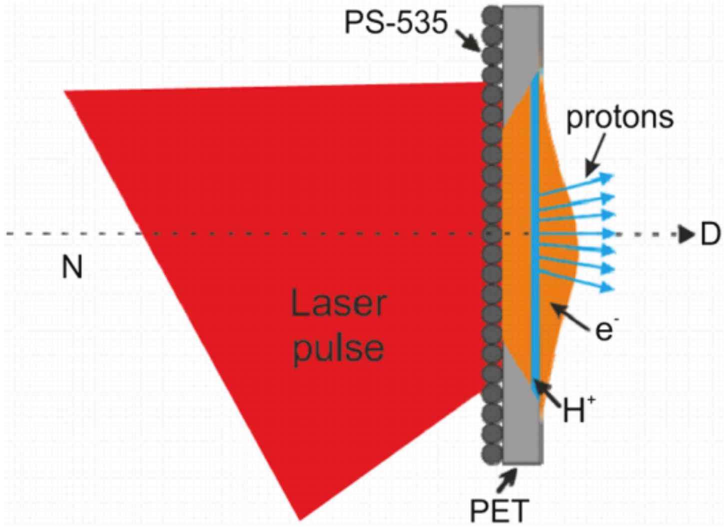

TP spectra

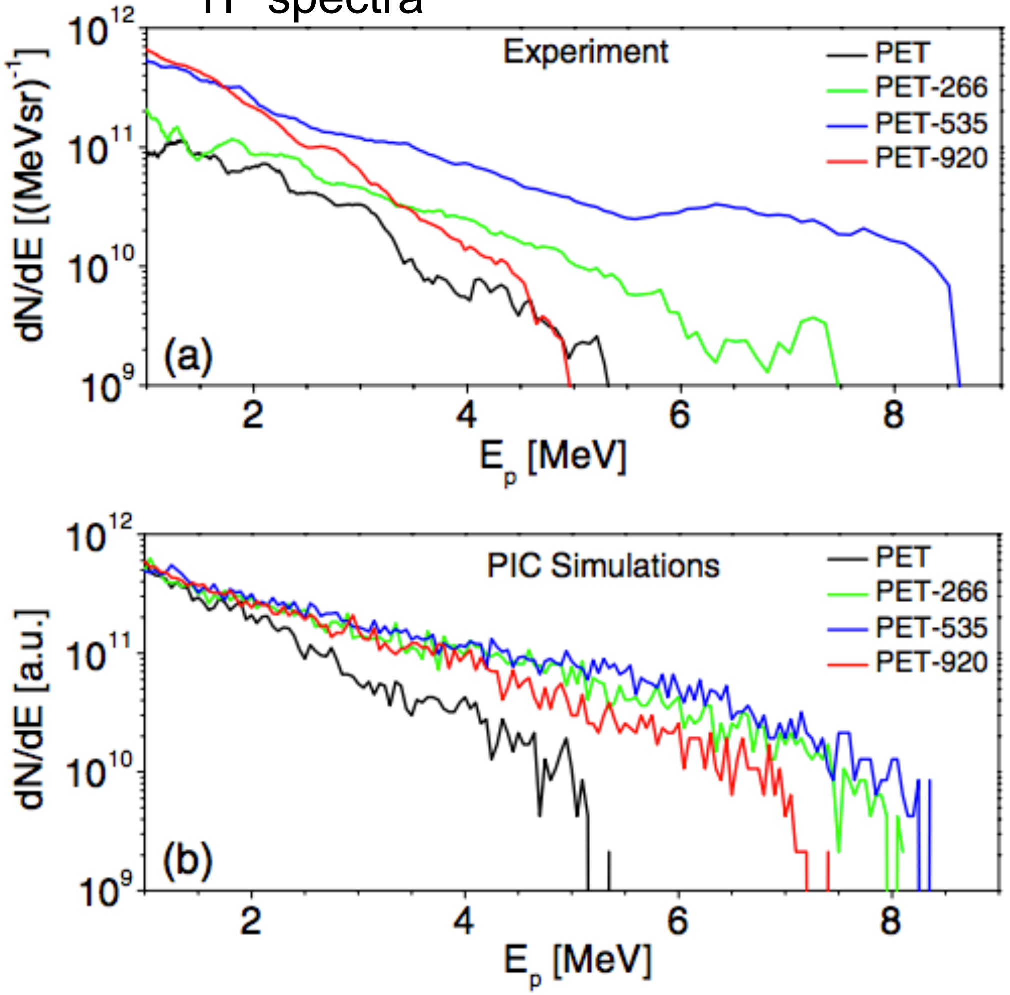

Proton energy distributions from analysis of TP spectra (a) and PIC simulations (b) for different irradiated targets. The vertical axis in (b) was rescaled in order to match the experimental values. The experimental cutoff energy for PET, PET-266, PET-535, PET-920 is 5.3, 5, 7.5, and 8.6 MeV, respectively. The PIC simulation cutoff energy for PET, PET-266, PET-535, PET-920 is 5.2, 7.2, 8, and 8.4 MeV, respectively.

100TW APRI System

t_L ~ 30fs
λ =805nm

Laser spot (FWHM) of 5μm dia.
(p-polarization, at 22.5º)

Laser energy ~ 2 J
Laser energy after PM ~ 1 J (~50%)
Contrast ~ 10^{11} (ps)
Peak Intensity ~ 5x10^{19} W/cm^2

Target Mylar 1μm
with nanosphere on front surface (266, 535, 920 nm)

Reduced mass target

S. Buffechoux *et al.*, PRL 105, 015005 (2010)

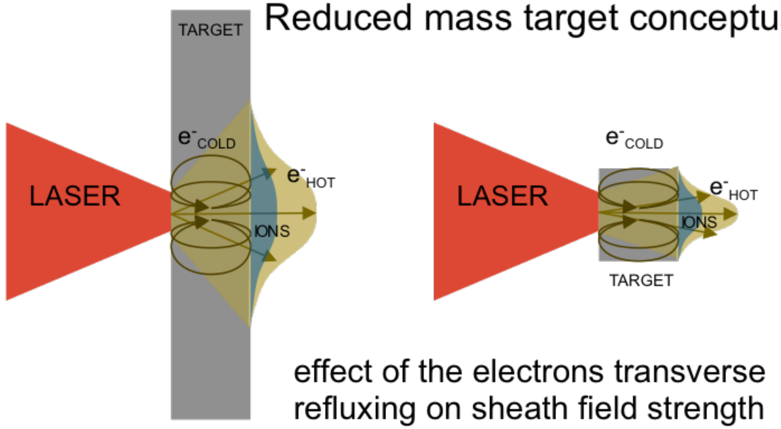

Reduced mass target conceptual

effect of the electrons transverse refluxing on sheath field strength

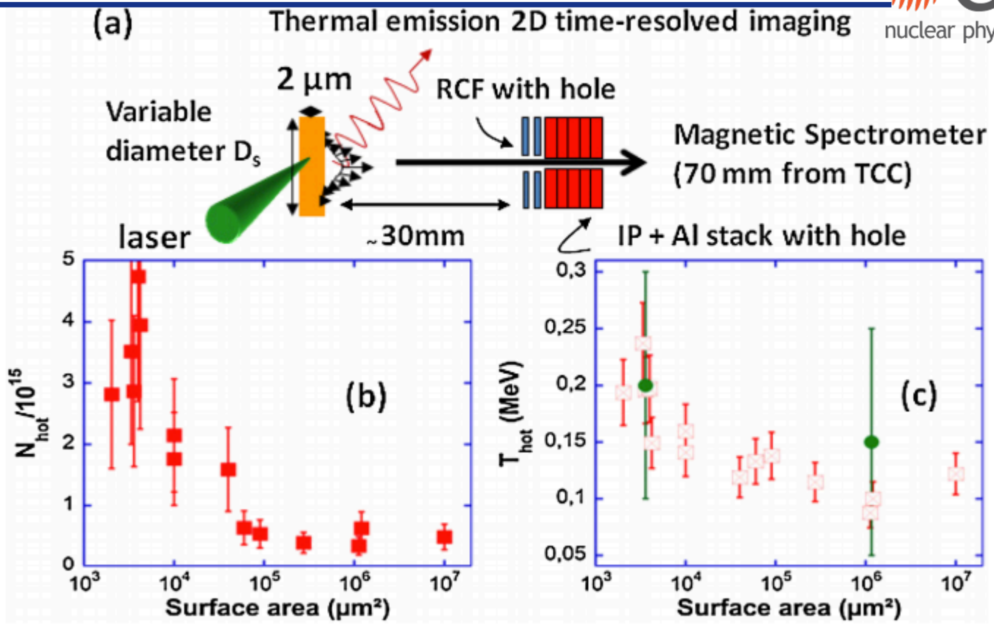

(a) Setup of the experiment.
(b) Effective number of hot electrons in the accelerating sheath N_{hot},
(c) effective hot electron temperature T_{hot} as a function of surface area.
Squares are extracted from the RCF measured proton spectra.

100 TW LULI System

t_L ~ 400fs
λ =1064nm doubled to 529nm
(for contrast improvement)

Laser spot (FWHM) of 6µm dia.
(s-polarization, at 45º, target centre)

Laser energy ~7 J,
Intensity ~ $2x10^{19}$ W/cm^2

Target Au 2µm (constant thickness)
with variable surface areas (few mm to 10s µm)

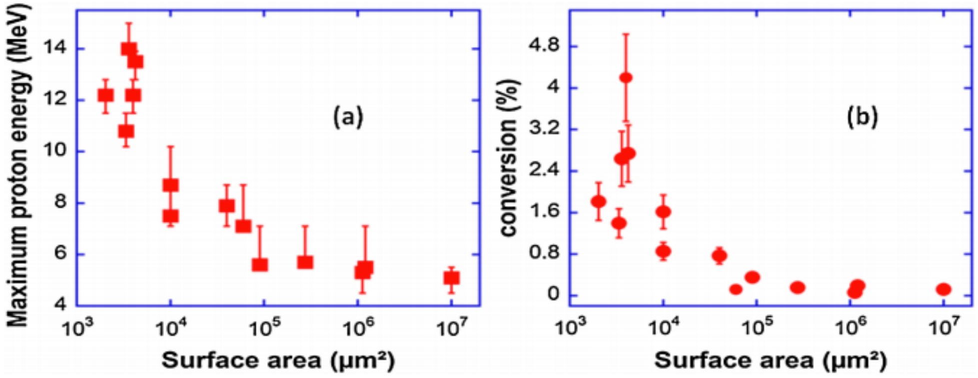

Data from RCF give (a) maximum proton energies for 2µm thick Au targets of various surface area
(b) laser-to-proton energy conversion efficiencies (for protons with energy >1.5 MeV) for the same targets.

Post-Acceleration

S. Kar et al., Nat. Com. 7, 10792 (2016)

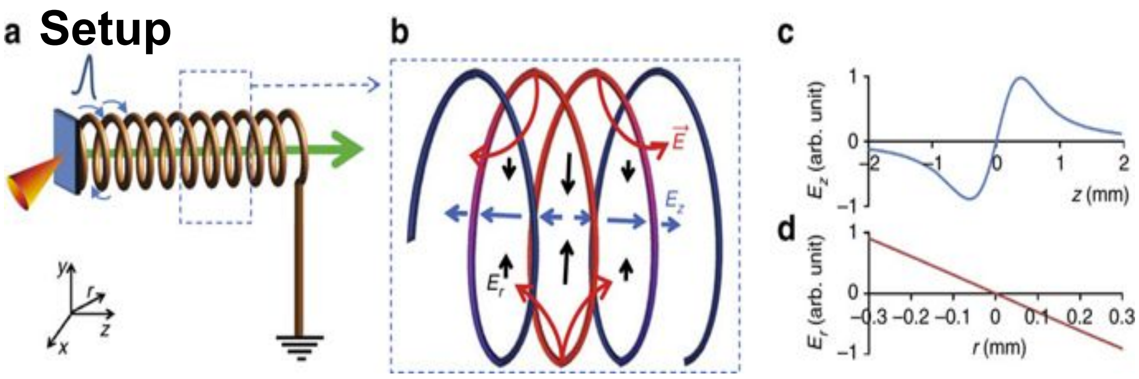

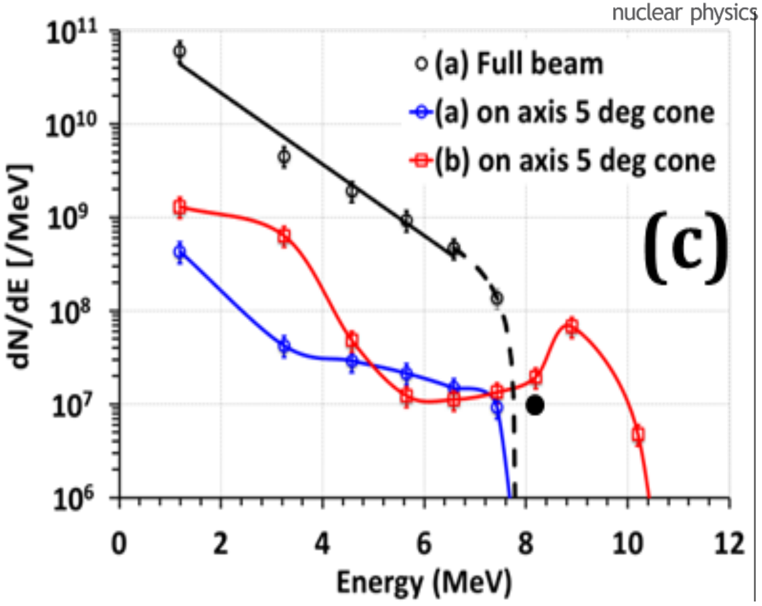

100TW ARCTURUS System

t_L ~ 30fs
λ =800nm

Laser spot (FWHM) of 4μm dia.

Laser energy ~3 J,
Intensity ~ 10^{20} W/cm^2

Target Au 10μm
Al Coil 100μm wire
int. dia. 700 μm
pitch 280 μm
length 8.7 mm

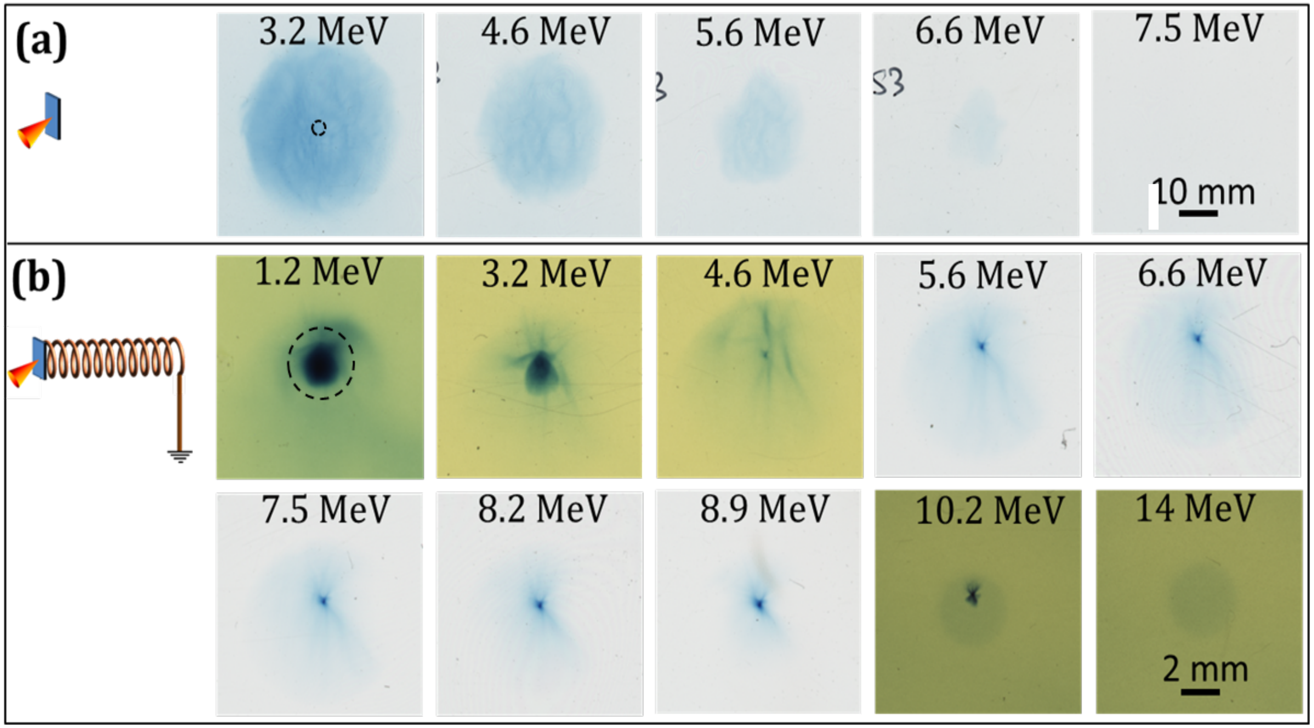

TNSA scaling law and state of the art

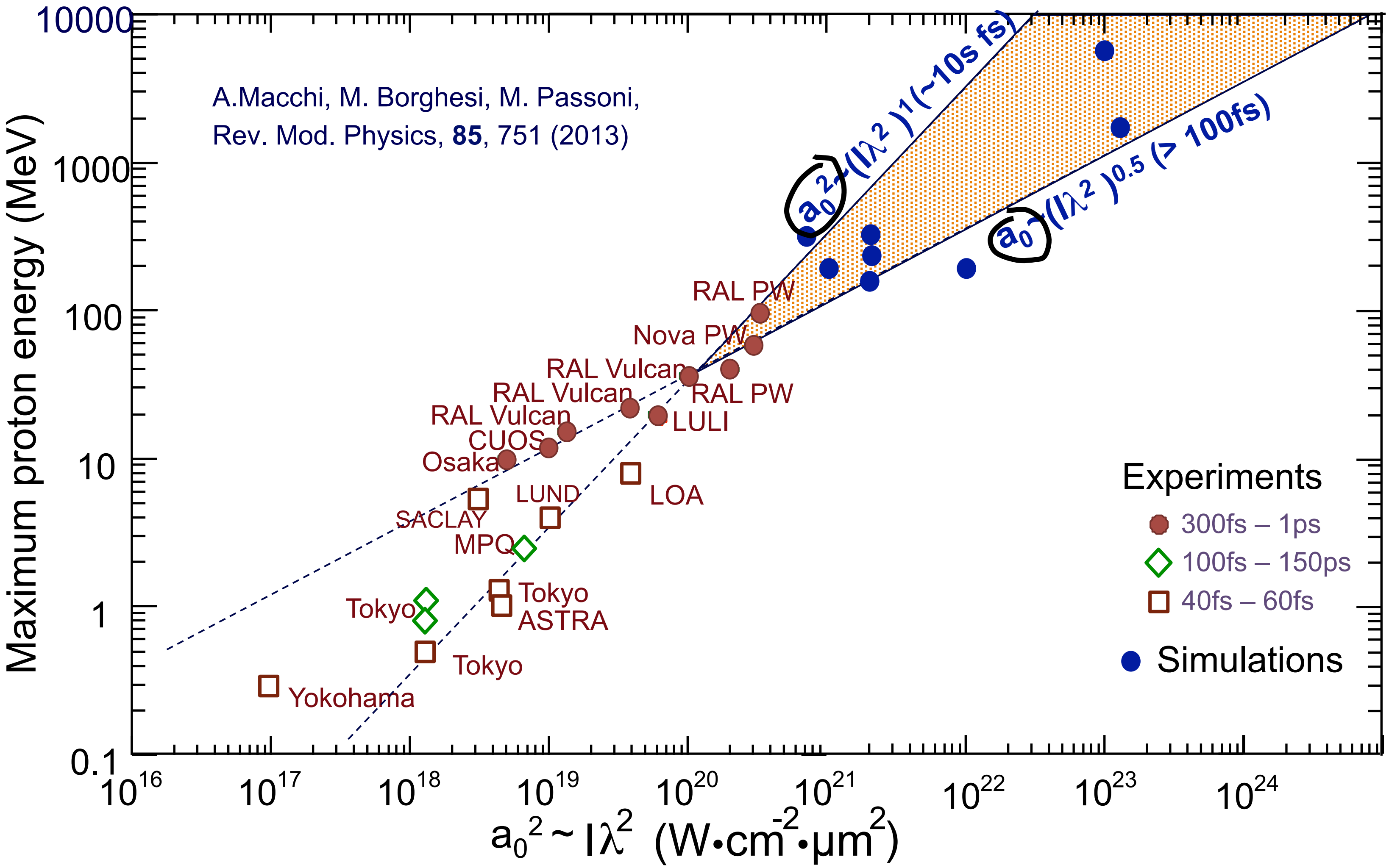

Maximum published energies: ~100 MeV

Acceleration more effective with higher energy, longer pulses, at equal intensities < 10^{20} W/cm^2

Effective on protons, less so on higher-Z species

TNSA scaling law and state of the art

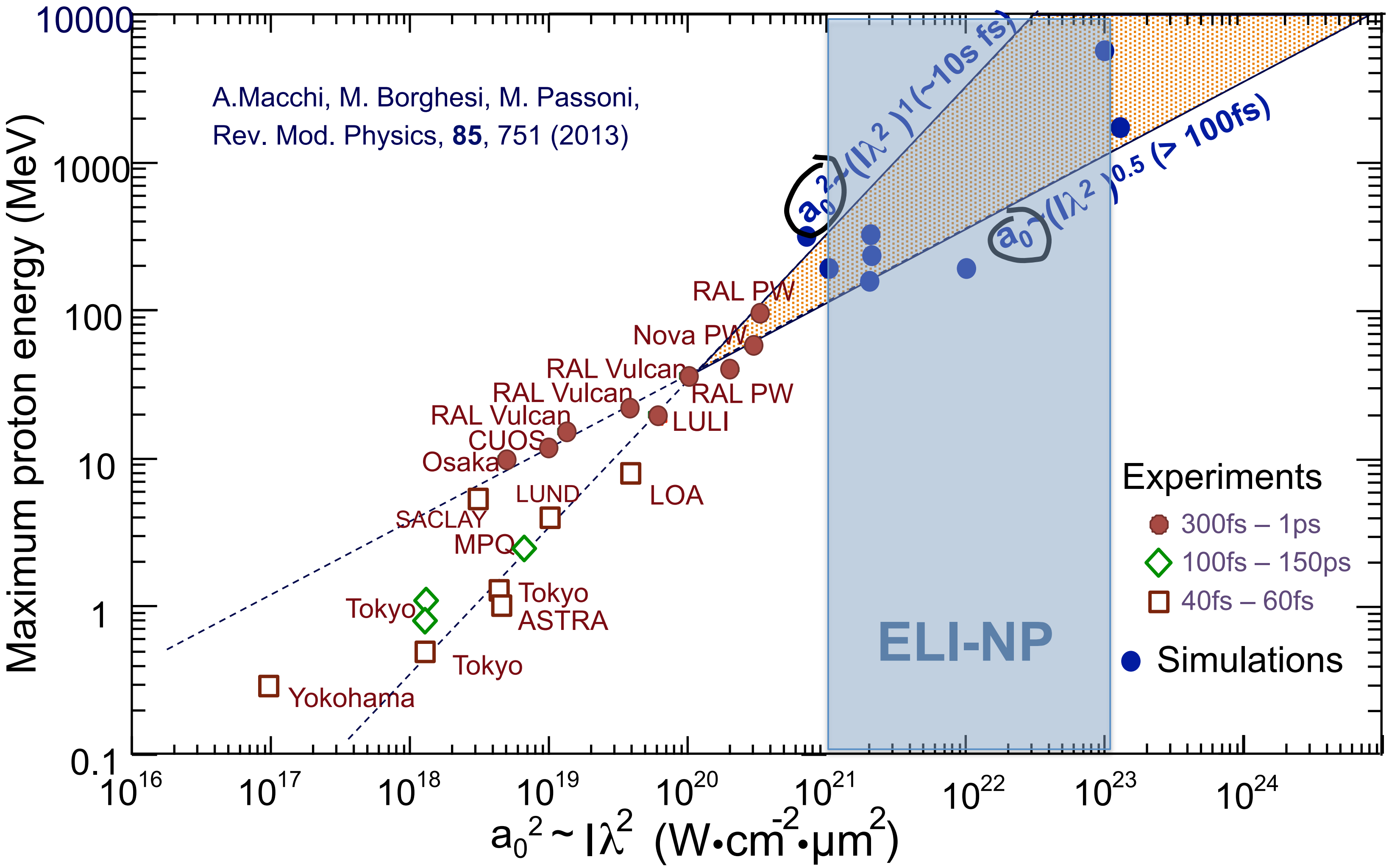

A.Macchi, M. Borghesi, M. Passoni, Rev. Mod. Physics, **85**, 751 (2013)

Maximum published energies: ~100 MeV

Acceleration more effective with higher energy, longer pulses, at equal intensities < 10^{20} W/cm^2

Effective on protons, less so on higher-Z species

Acceleration mechanisms

Sheath (surface) acceleration:
(in micron-thick targets)

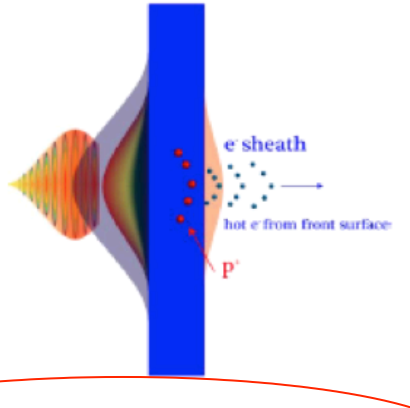

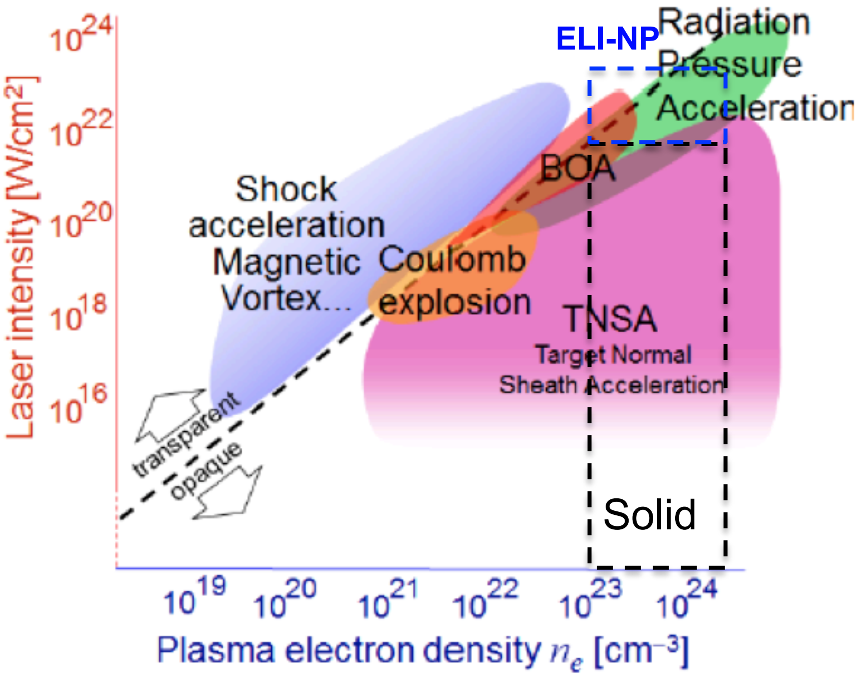

Volumetric acceleration:
(in nanometre-thick targets)

Radiation pressure acceleration

Hole-Boring

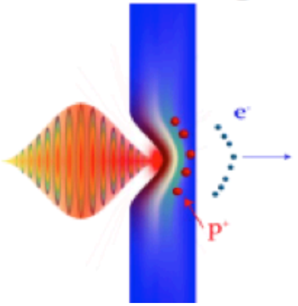

Light Sail

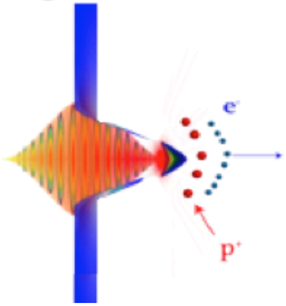

Relativistic transparency
(BOA) regime

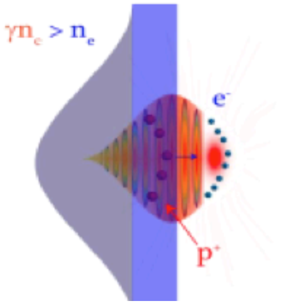

RPA characteristics and issues

Why do we want to go for RPA?

Collimated beam

Narrow-band spectrum (whole-foil acceleration)

High conversion efficiency

Short bunch duration

Faster scaling with intensity

How can we do it?

Ultra-thin foil

Shaping the laser focal spot

Solving detrimental issues

Acceleration mechanisms

Radiation pressure acceleration

Hole-Boring

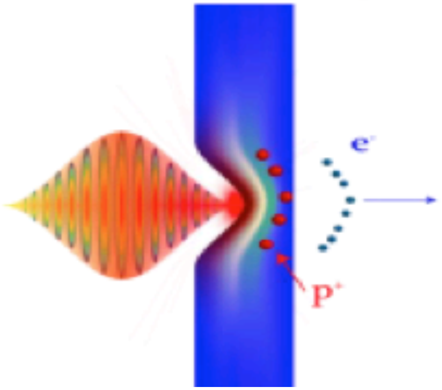

Light Sail

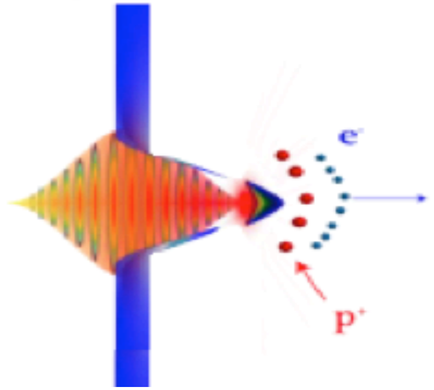

Relativistic transparency (BOA) regime

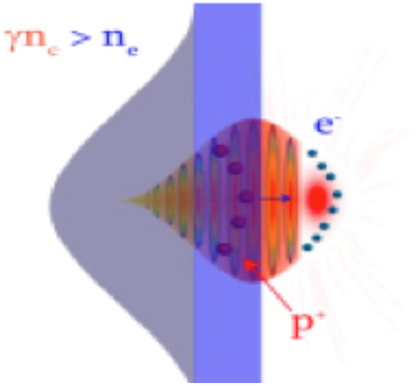

$$\tau < t_{HB}$$

τ = laser pulse

t_{HB} = time to go through

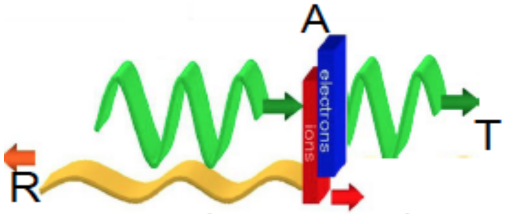

$$(R + T + A) = 1$$

$$F_R = (2R + A)S\frac{I}{c}$$

Ion velocity

Surface Area

$$\Rightarrow v_i = \frac{(2R + A)\tau}{m_i n_i d}\frac{I}{c} \propto I\tau/\eta$$

$\eta = m_i n_i d$, Areal density

$E_{\max} \sim (I_L \tau/\eta)^2$ (non-relativistic)

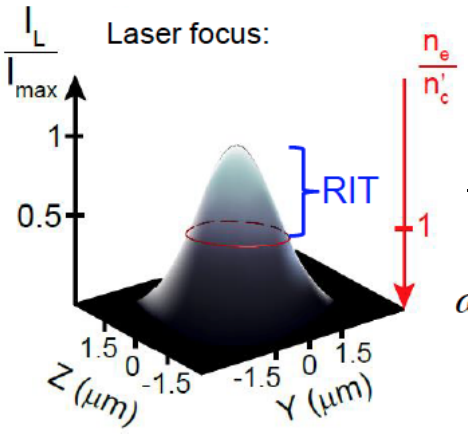

Plasma frequency

$$\omega_p = \sqrt{\frac{e^2}{\varepsilon_0}\frac{n_e}{\gamma m_e}}$$

Decrease in plasma frequency near the peak of the focus produces Relativistically Induced Transparency over a diameter of a few times the laser wavelength

Radiation Pressure Acceleration

Kar, S., et al., Phys. Rev. Lett, 109, 185006 (2012)

Schematic of the experimental setup.

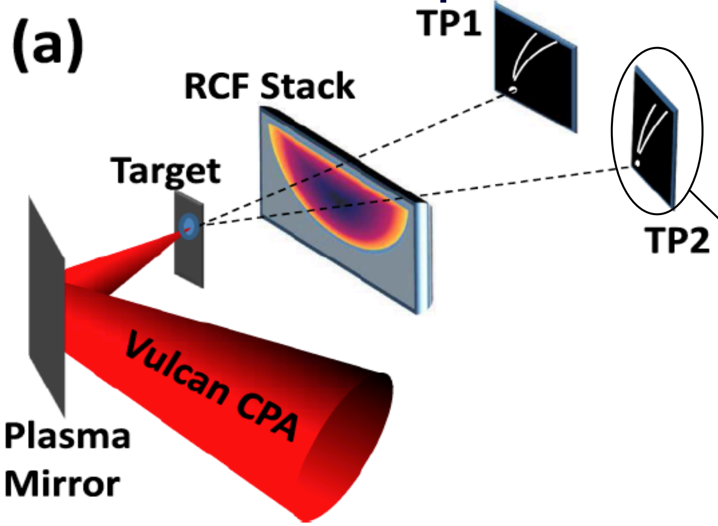

Detector structure

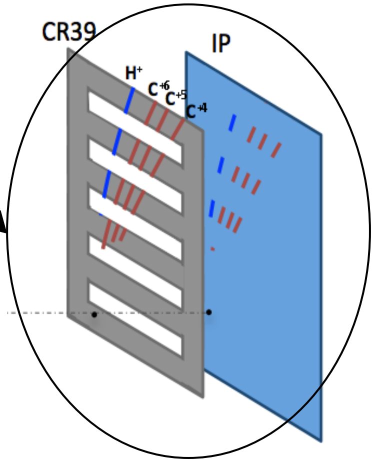

TP 1 – typical signal

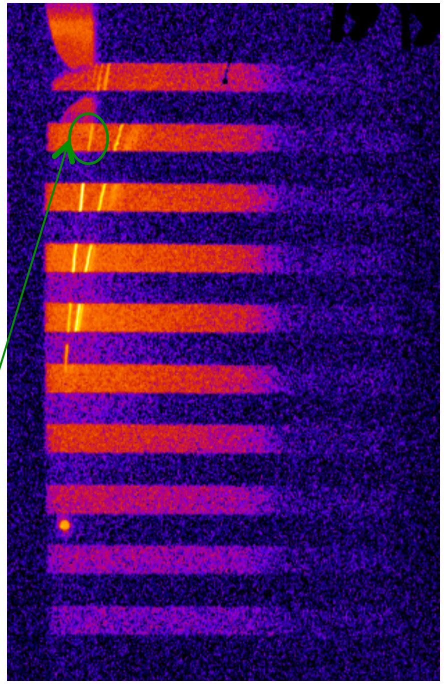

CR39 trace

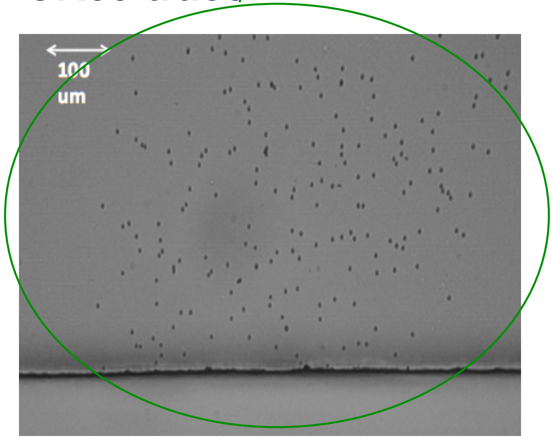

1PW CLF Vulcan System

t_L ~ 800fs
λ =1054nm

Laser spot (FWHM) of 30µm dia.
(p-polarization, at 45º)

Laser energy main up to 600J
Laser energy after PM up to 450 J (~75%)
Contrast ~ 10^{11-12} (ps)

Intensity main ~ 1-3x10^{20} W/cm^2

Cu target 50-500 nm thick

Radiation Pressure Acceleration

B. M. Hegelich, et al.,, Nature **439**, 441 (2006).

A. Henig et al., Phys. Rev. Lett. **103**, 245003 (2009)

Kar, S., Kakolee, K. F., Qiao, B., Macchi, A., Cerchez, M., **Doria, D.**, et al., Phys. Rev. Lett, **109**, 185006 (2012)

Doria, D. et al., RSI. **86** 12, 123302 (2015)

Difficulties in extending scaling due to transparency and instability issues

Thomson parabola spectra

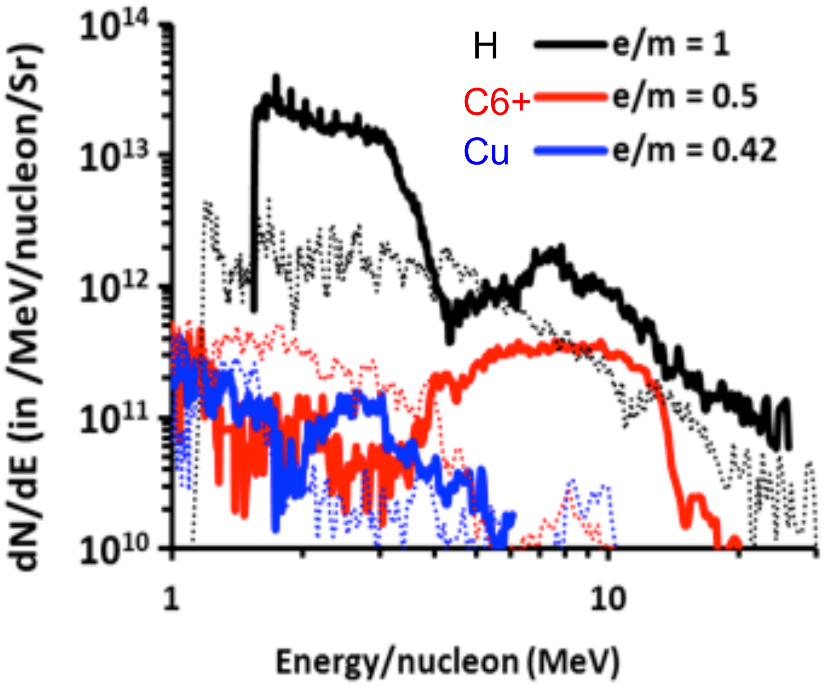

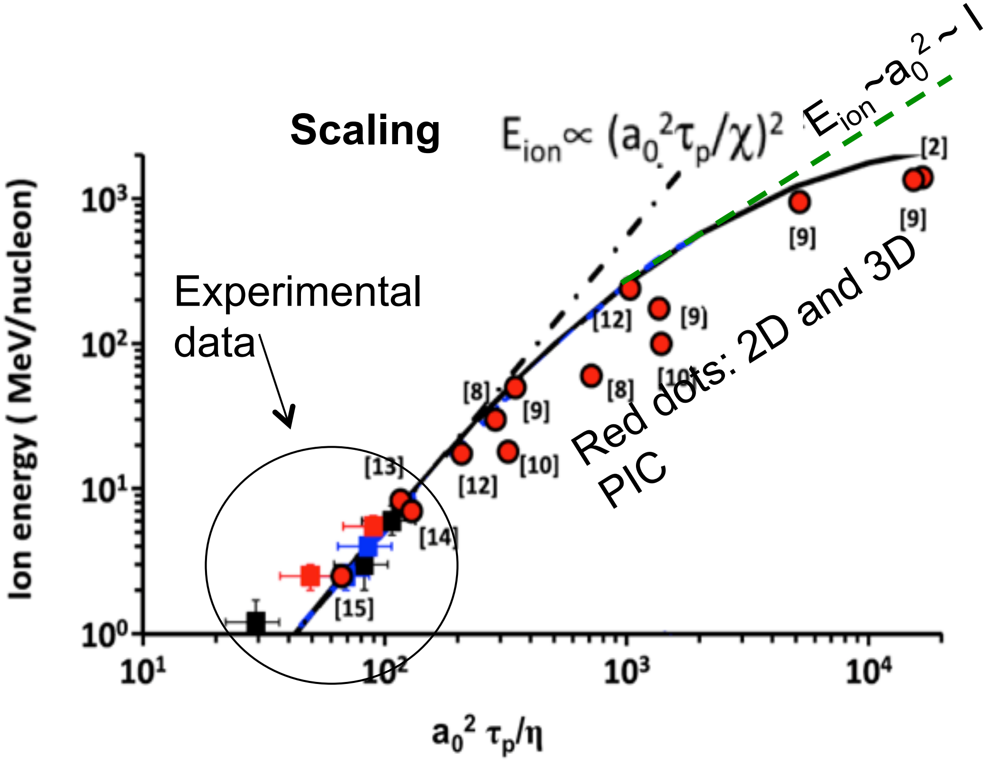

Targets thicker than 500nm show standard continuous, exponential spectra (TNSA)

Peaks observed regardless of laser polarization (LP or CP)

Hybrid scheme where TNSA and RPA cohesist

Theory described in B. Qiao et al, PRL, 108, 115002 (2012)

Issues for RPA

Rayleigh-Taylor instability (RTI)

Sgattoni, A. et al., PRE, **91** 1, 013106 (2015)

PIC code ALADYN and PICCANTE

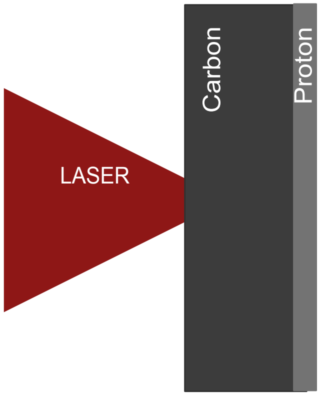

$L_C = \lambda$, $n_C = 64 n_c$
$L_P = \lambda/22$, $n_P = 8 n_c$

Laser Intensity $a_0 = 198$

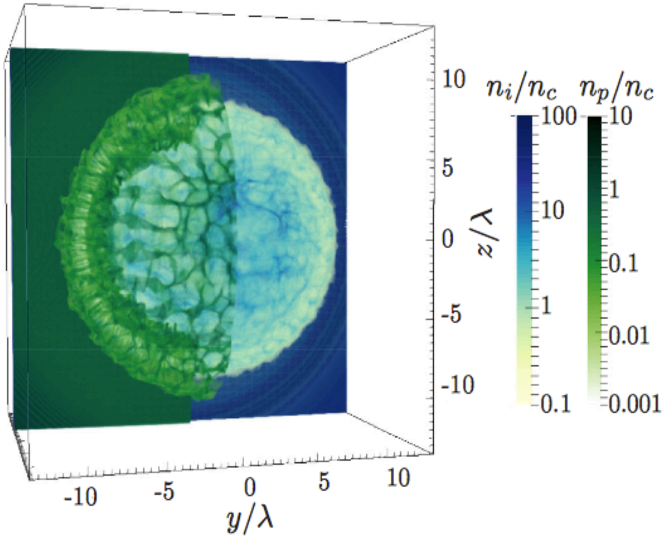

FIG. 5. (Color online) A 3D snapshot image of the density of both proton (dark green tones) and carbon (light blue tones) densities at $t = 30T$. In order to make the carbon ion density visible, the proton density is shown only on the left part ($y \geqslant 0$) of the image.

The early growth of the RTI does not prevent reaching high energy of ions in the radiation pressure-dominated regime.

The ion beam becomes strongly modulated and non-uniform as a consequence of the RTI

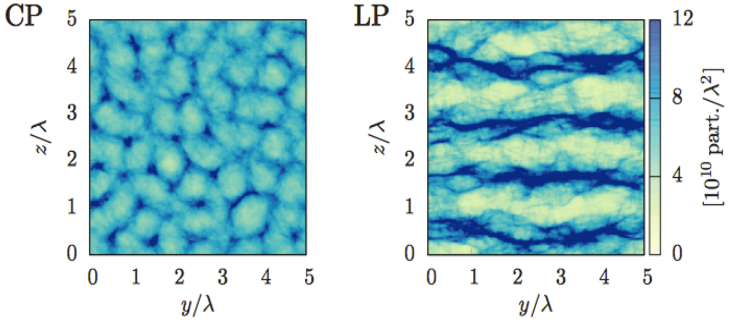

FIG. 6. (Color online) Areal density of carbon ions at $t = 15T$ in 3D simulations with the same parameters as in Fig. 5 but for a plane wave, for circular (CP) and linear (LP) polarization.

Simulation of RPA regime

EPOCH Simulations for Linear and Circular polarization

Target 10nm Carbon

Intensity = $4.9\text{x}10^{20}$ W/cm^2

Time 0fs

Electron density

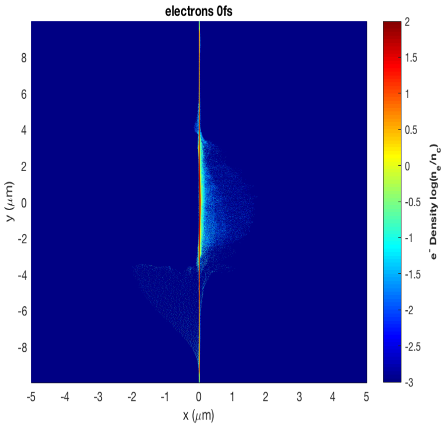

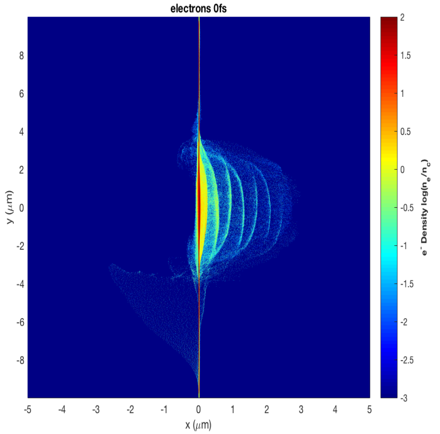

- **EPOCH 2D**
- Resolution 5x6.6nm
- -5μm → 50 μm for x (propagation)
- -10 μm → +10 μm for y
- 11000 x 3000 cells
- 200 particles per cell

Laser

- 3 μm FWHM focal spot
- 40fs FWHM pulse width
- λ = 800nm
- Normal incidence

Target

- Carbon – 2g/cm^3
- Bulk is pure Carbon ne=350nc
- Rear Low density Proton Layer 12.5nm - Mimics contaminant layer , ne=10nc
- nc=$1.75\text{x}10^{24}$ g/cc

Ey - field

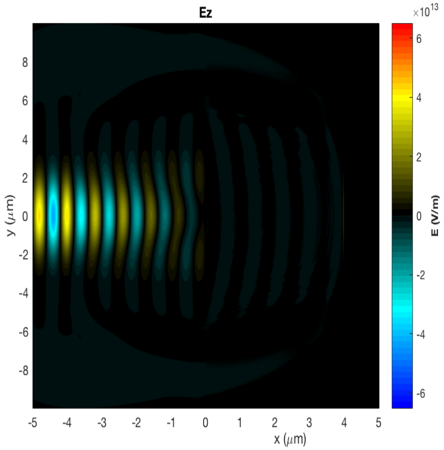

C-pol

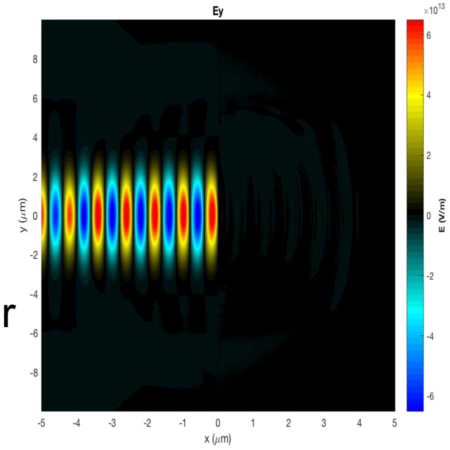

L-pol

Simulation of RPA regime

EPOCH Simulations for Linear and Circular polarization

Target 10nm Carbon

Intensity = 4.9×10^{20} W/cm^2

Time 20fs

Electron density

Ex - field

Ey - field

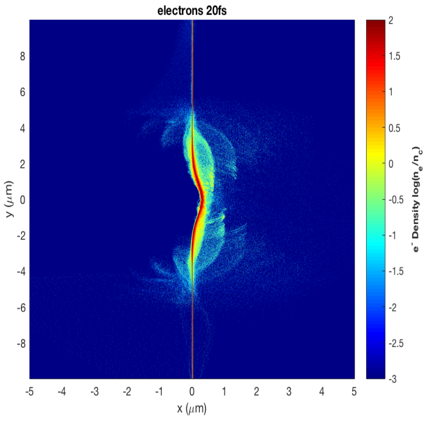

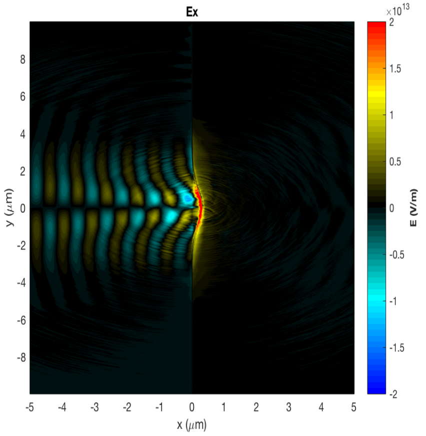

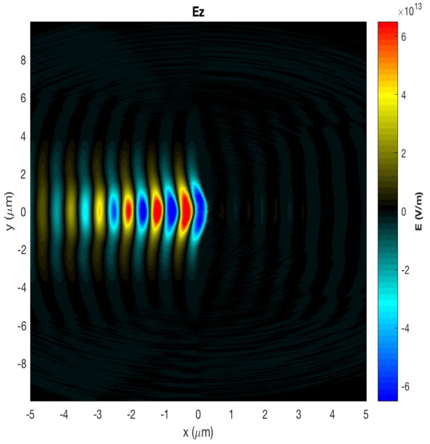

C-pol

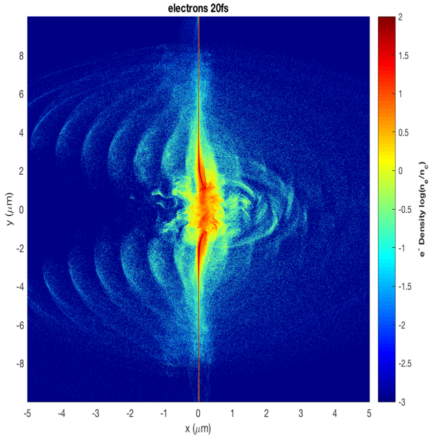

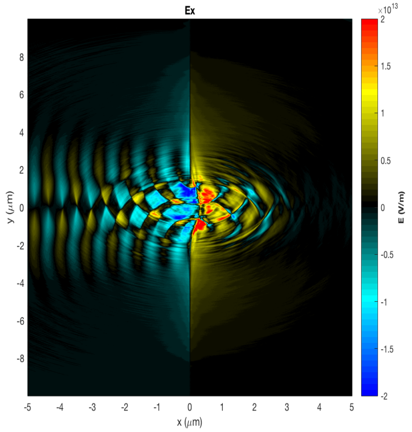

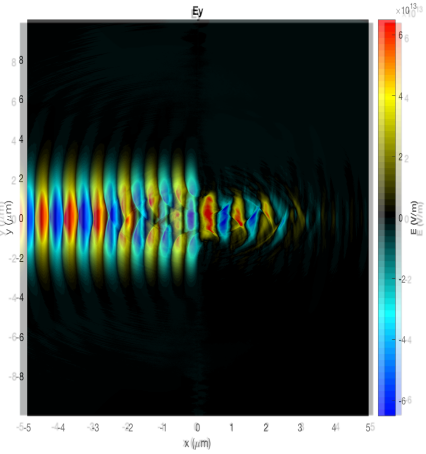

L-pol

Simulation of RPA regime

EPOCH Simulations for Linear and Circular polarization

Target 10nm Carbon

Intensity = 4.9x10^{20} W/cm^2

Time 30fs

Electron density

Ex - field

Ey - field

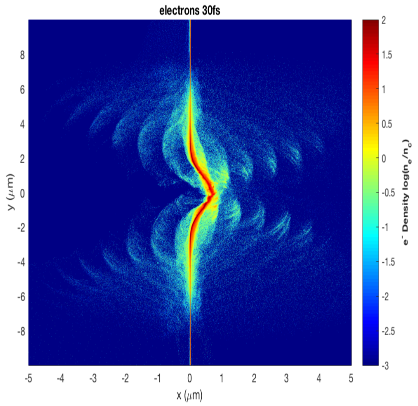

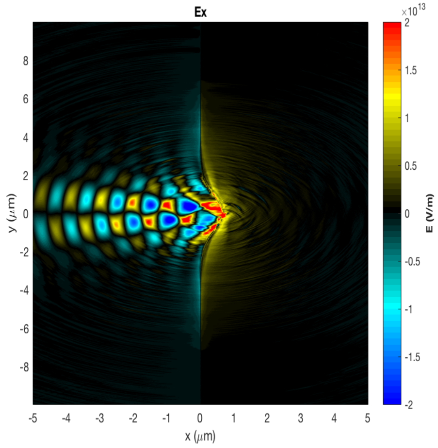

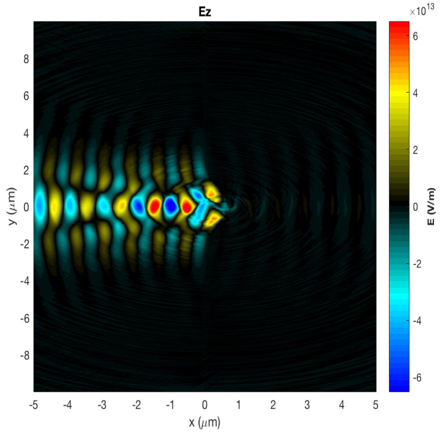

C-pol

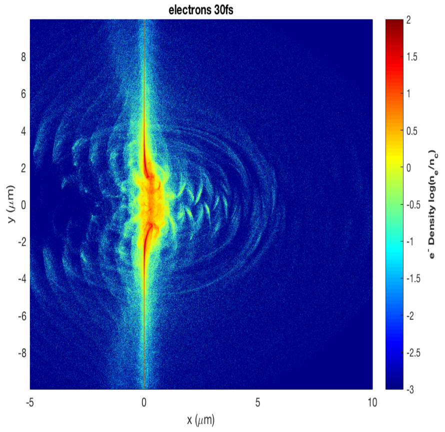

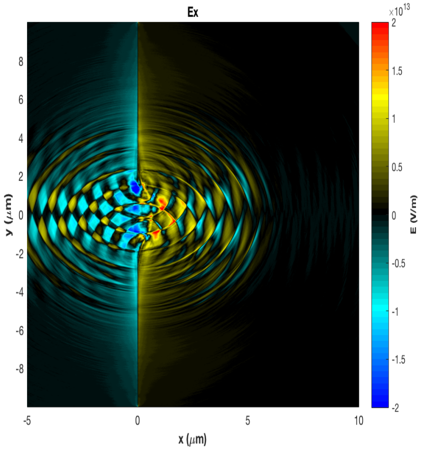

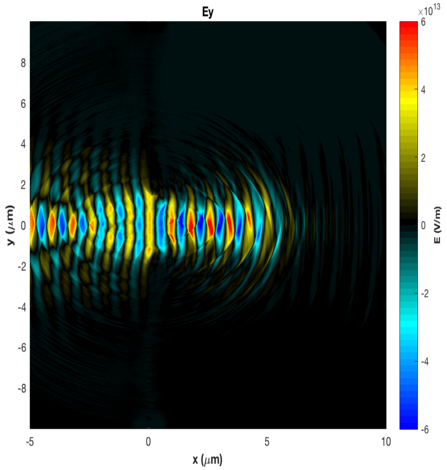

L-pol

Simulation of RPA regime

EPOCH Simulations for Linear and Circular polarization

Target 10nm Carbon

Intensity = 4.9×10^{20} W/cm^2

Time 40fs

Electron density

Ex - field

Ey - field

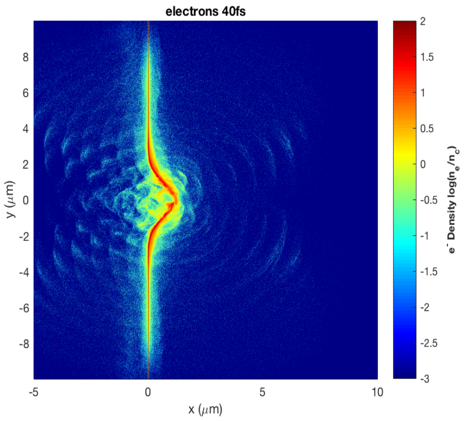

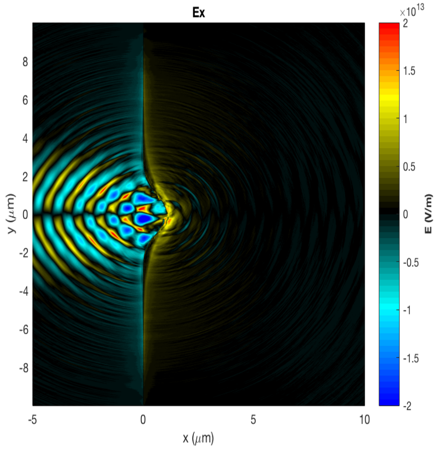

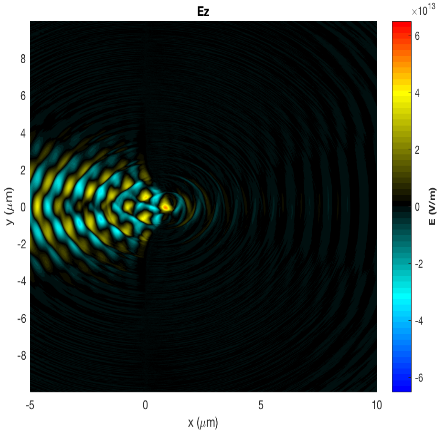

C-pol

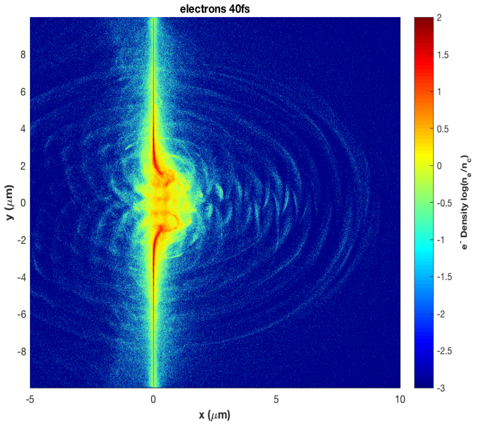

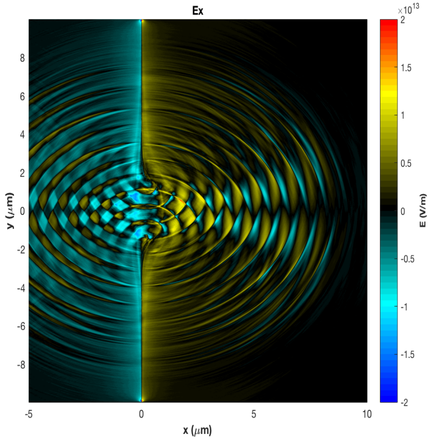

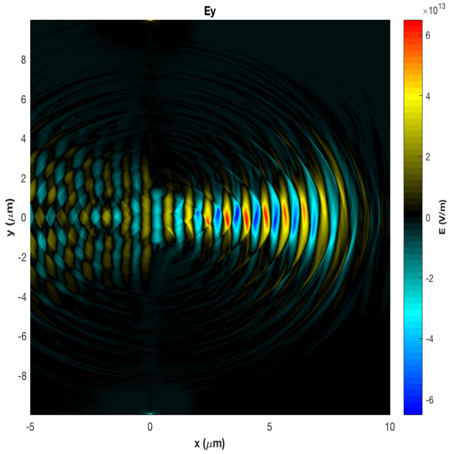

L-pol

Simulation of RPA regime

EPOCH Simulations for Circular polarization

Targets 10nm and 5nm Carbon

Intensity = 4.9×10^{20} W/cm^2

Time 20fs

10nm C

Electron density

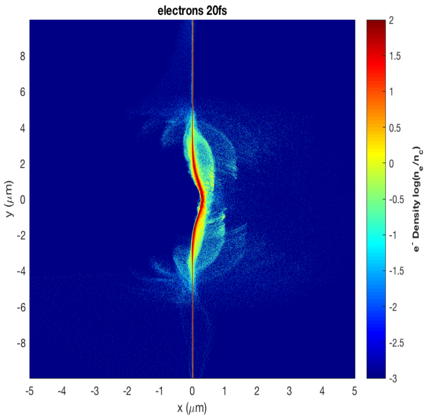

Ex - field

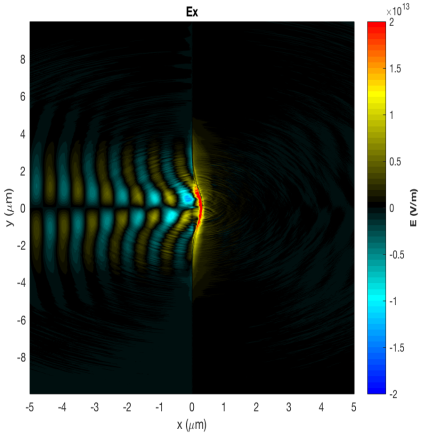

Ey - field

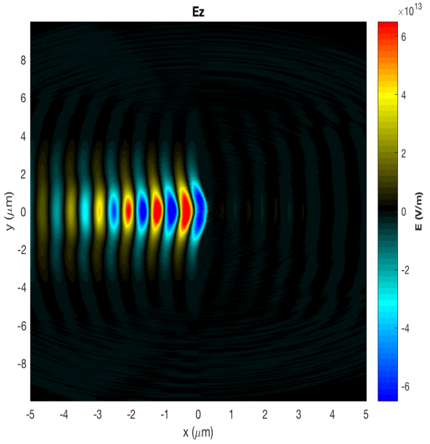

C-pol

5nm C

Electron density

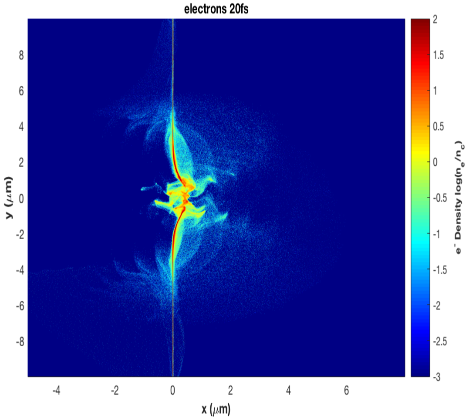

Ex - field

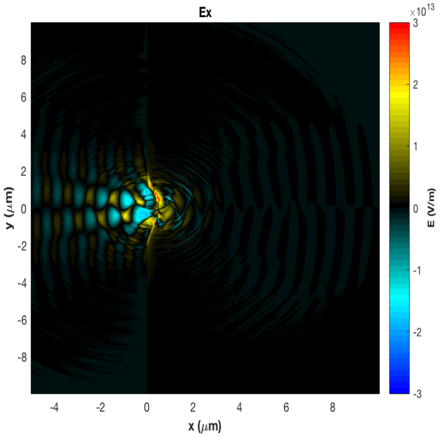

Ey - field

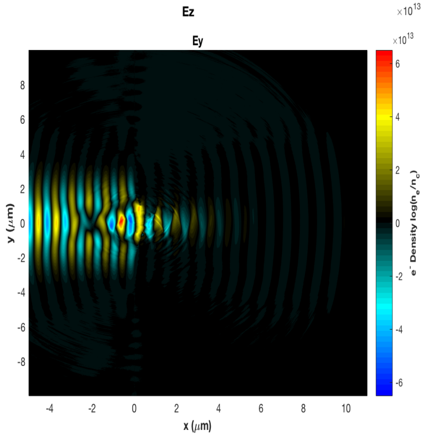

C-pol

Experimental Results on Light Sail regime of RPA

Scullion, C., ***Doria, D.**, et al., PRL 2017

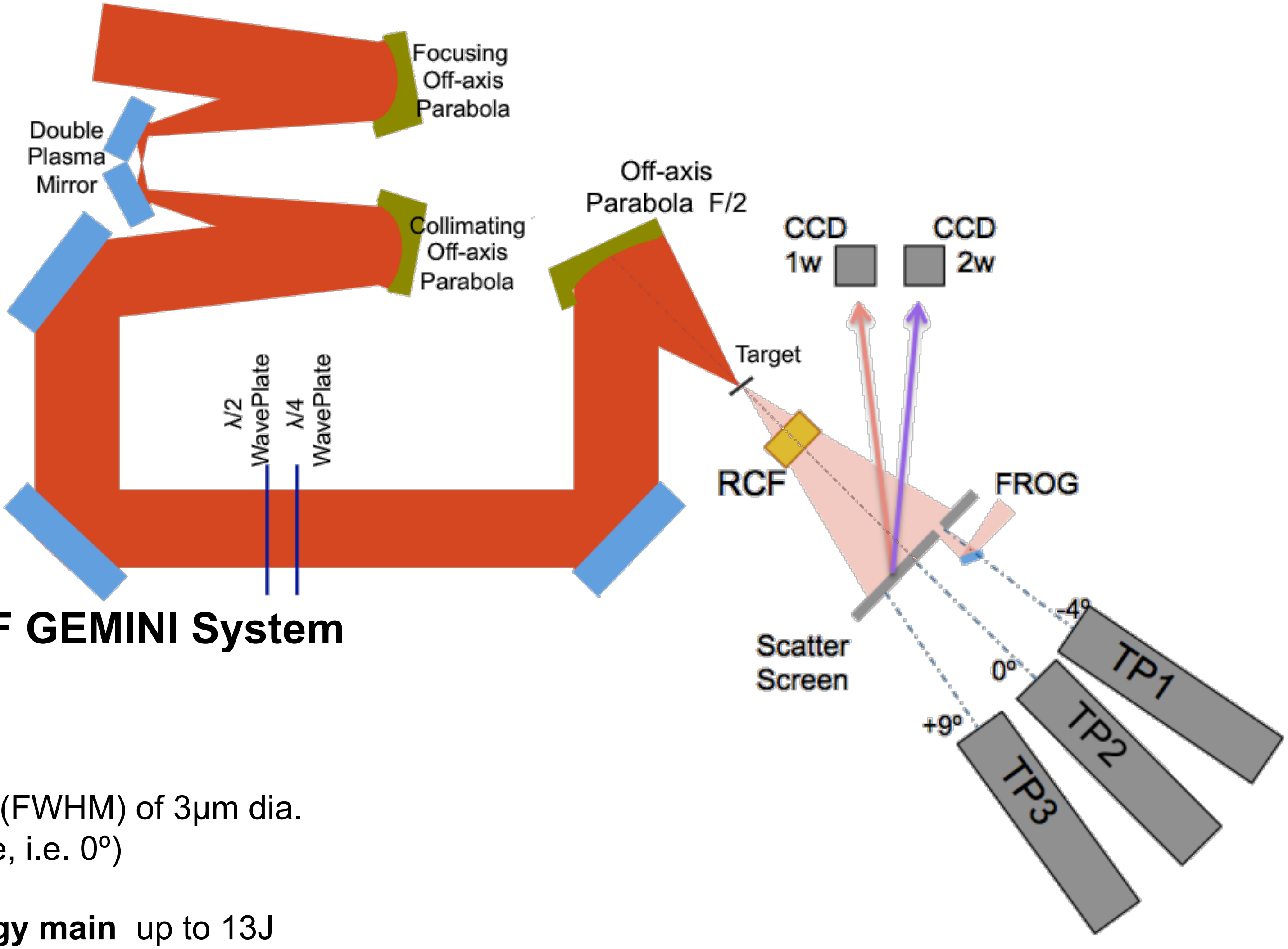

400TW CLF GEMINI System

t_L ~ 40fs
λ = 800nm

Laser spot (FWHM) of 3μm dia.
(S-incidence, i.e. 0°)

Laser energy main up to 13J
Laser energy after PM up to 6.5 J (~50%)
Contrast ~ 10^{12} (ps)
Intensity main ~ 4.9×10^{20} W/cm^2

C target 2-100 nm thick

Experimental Results on Light Sail regime of RPA

Carbon Spectra

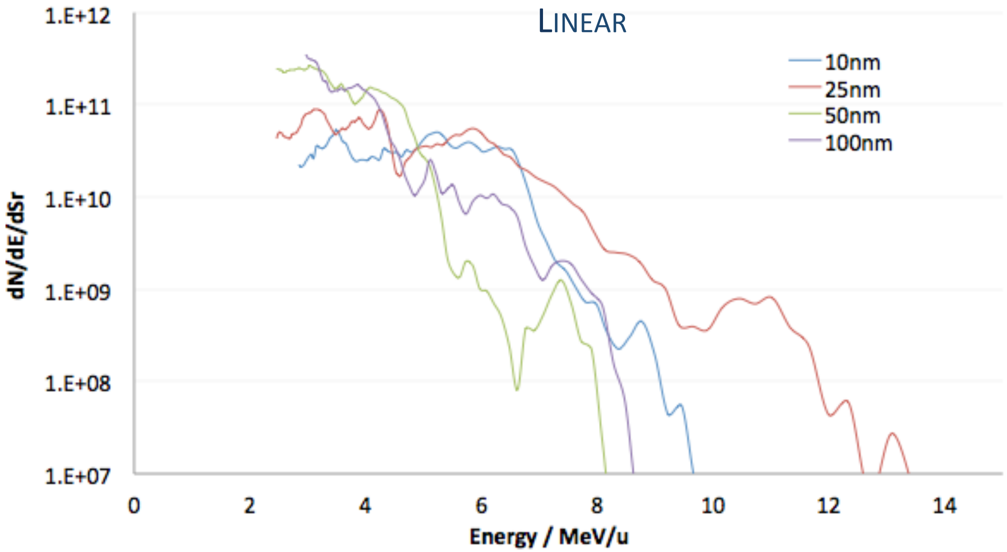

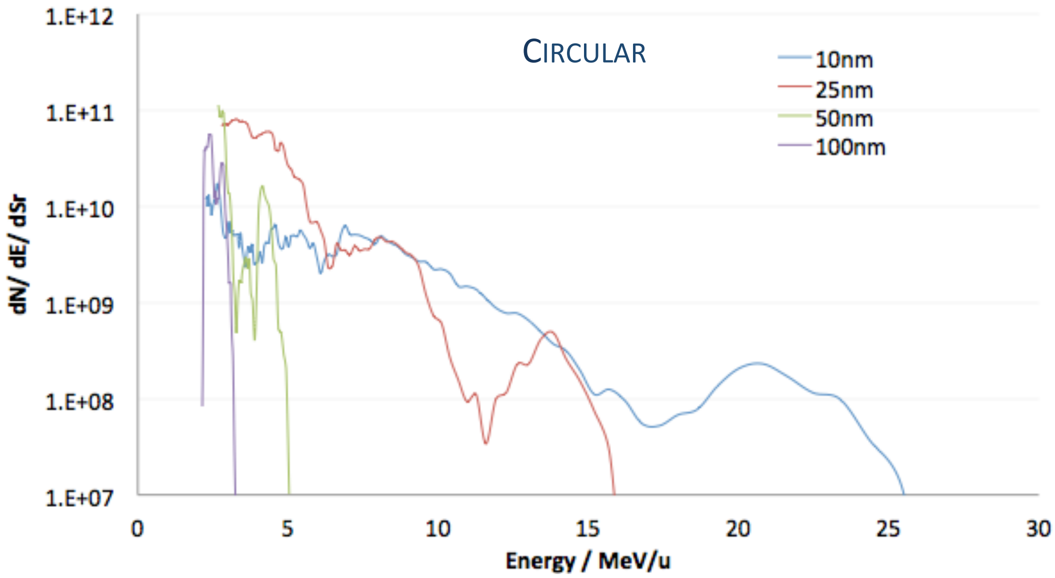

THOMSON PARABOLA

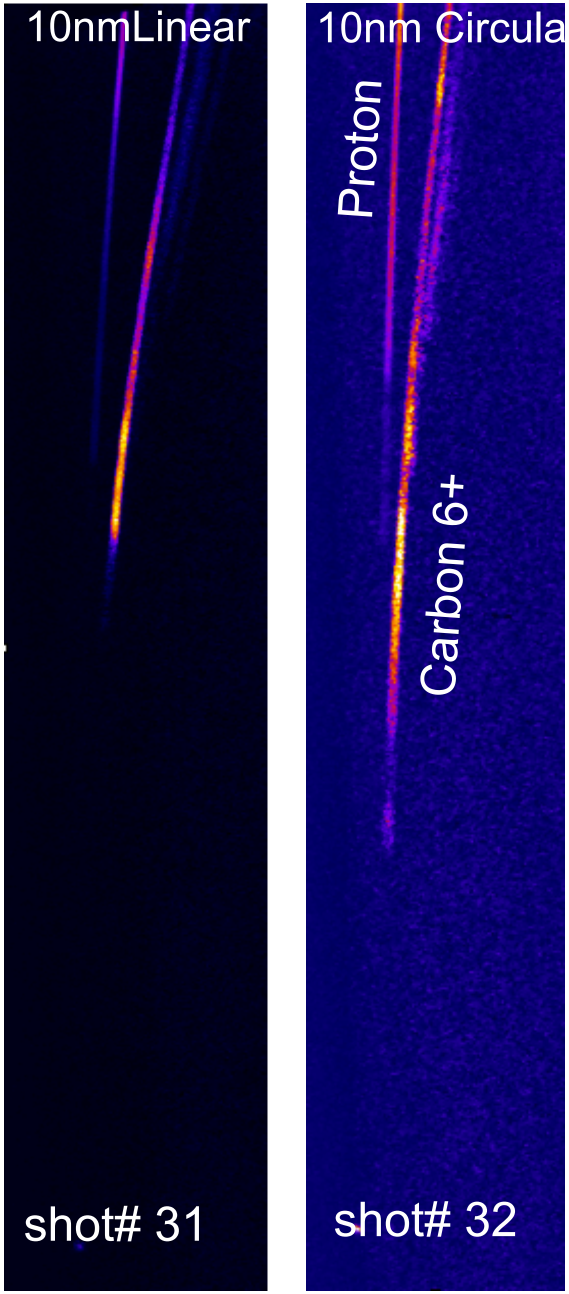

Experimental Results on Light Sail regime of RPA

Carbon Spectra

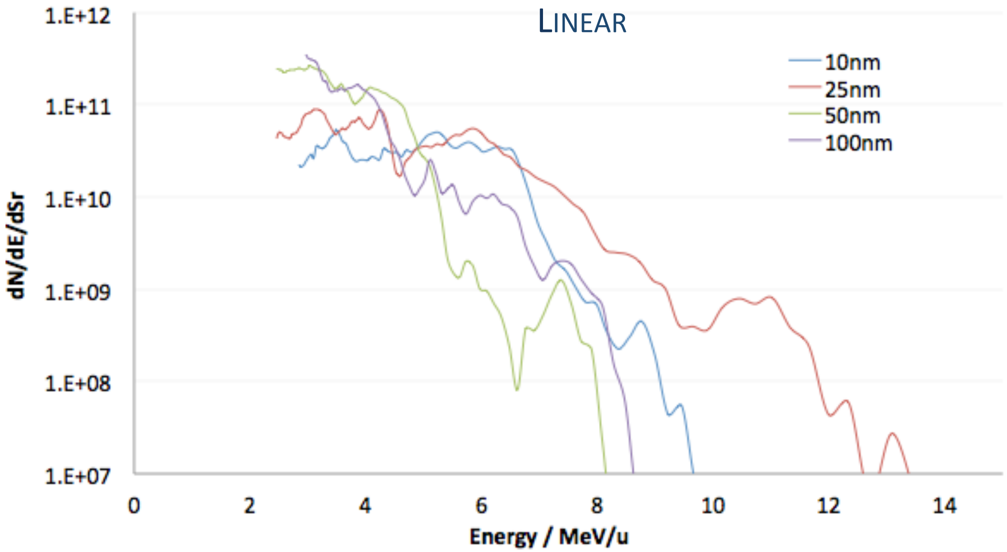

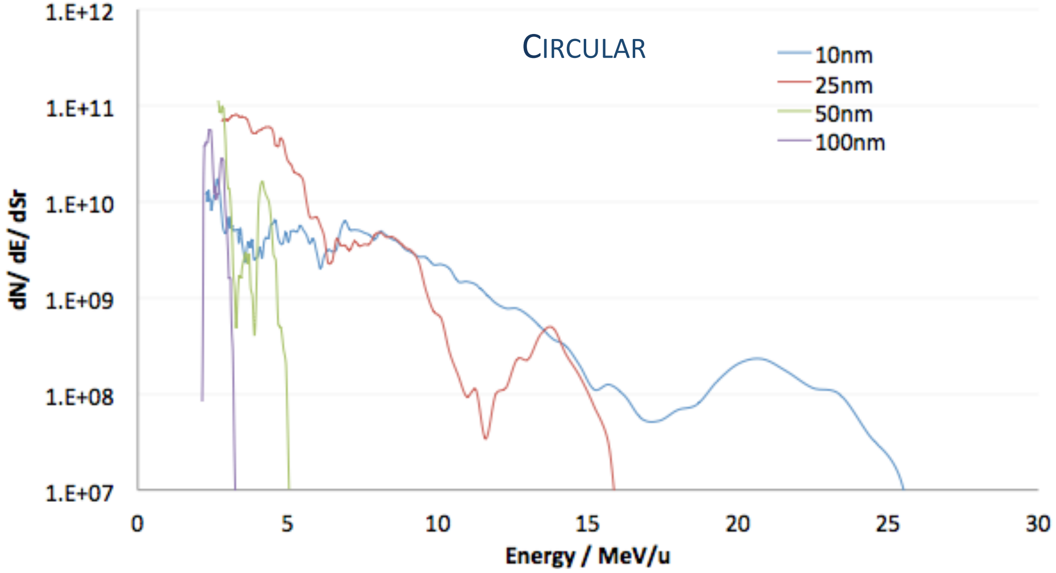

THOMSON PARABOLA

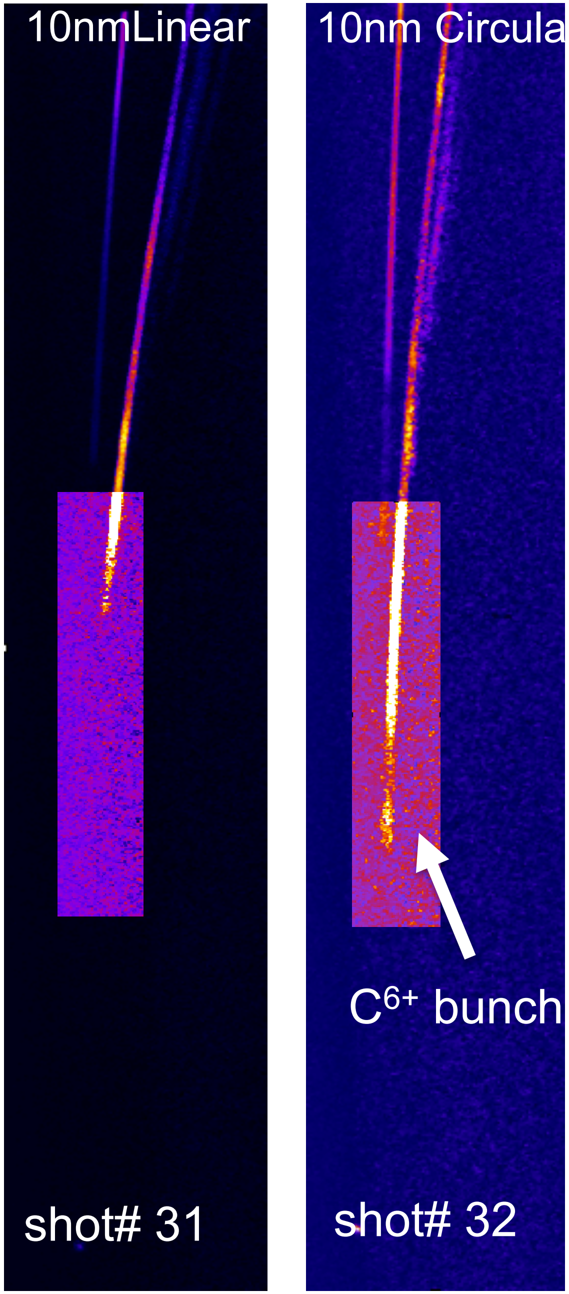

Experimental Results on Light Sail regime of RPA

Ion energy versus target thickness and polarization

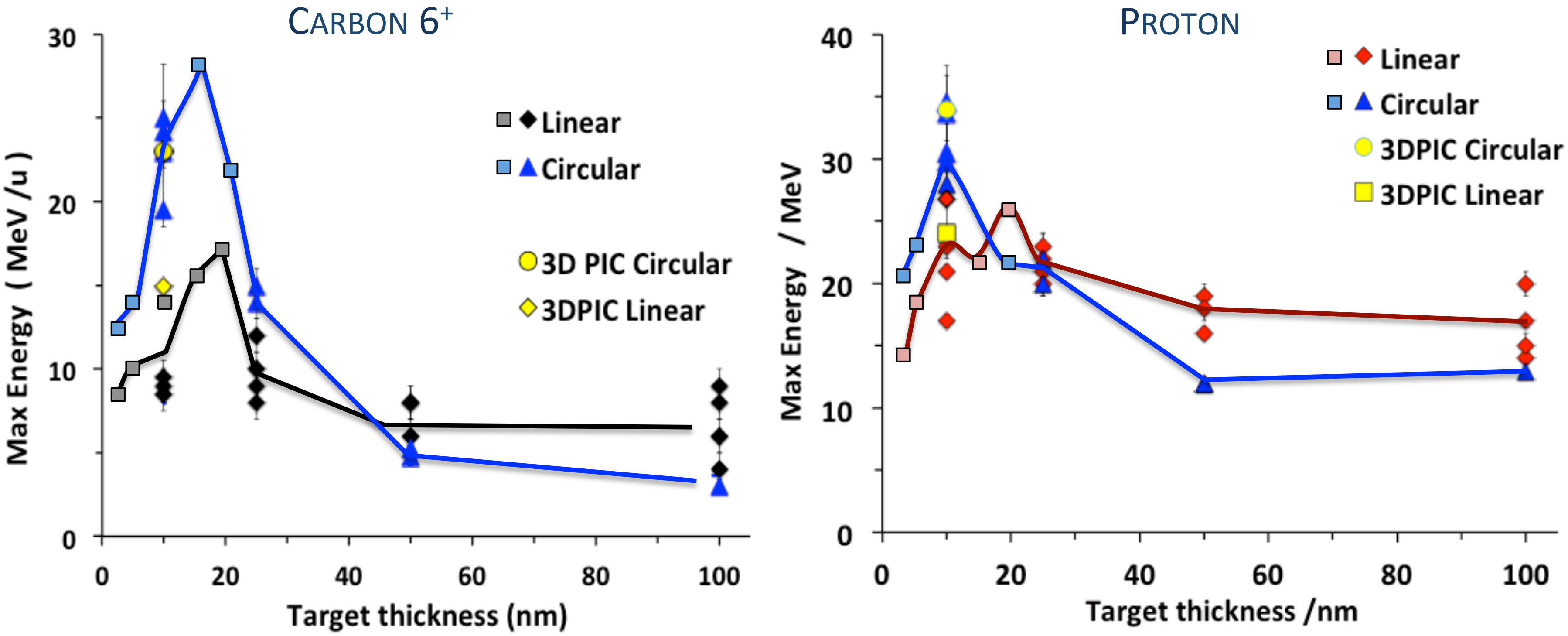

- First evidence of polarization dependence for high energy ions from thin foils – evidence of a transition to RPA
- Evidence of transparency and other issues

C. Scullion, **D. Doria** *et al* Phys. Rev. Lett. **119**, 054801 (2017)

Experimental Results on Light Sail regime of RPA

Effect of polarization on ion energy

I = 5×10^{20} W/cm^2

15nm C-a

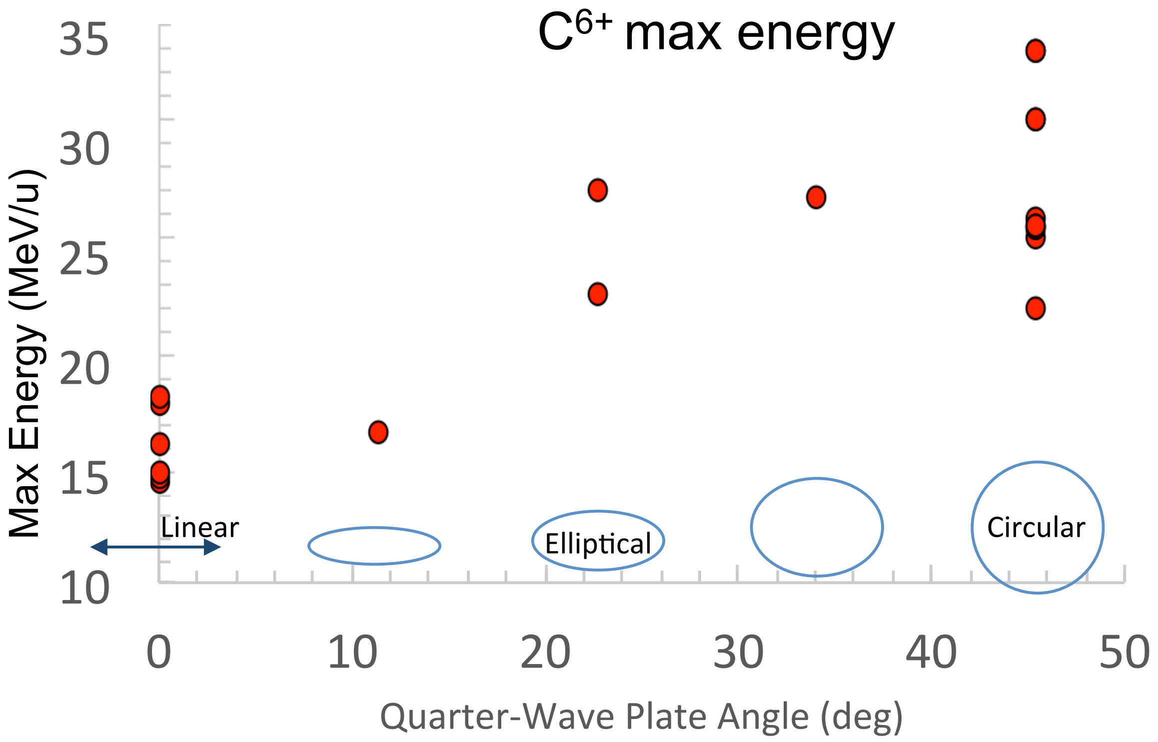

Radiation pressure

$$x(\tau) = \underbrace{\frac{ca_0^2}{4}\tau}_{\text{Circular}} + \underbrace{\frac{ca_0^2}{4}\frac{1}{2\omega}\sin(2\omega\tau)}_{\text{Linear}}$$

Experimental Results on Light Sail regime of RPA - Issues

RTI and Transparency signatures

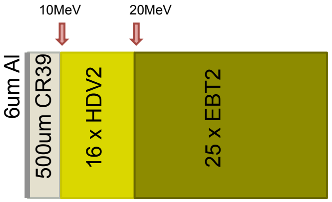

RCF/CR39 STACK

PROTON PROFILE USING RADIOCHROMIC FILM

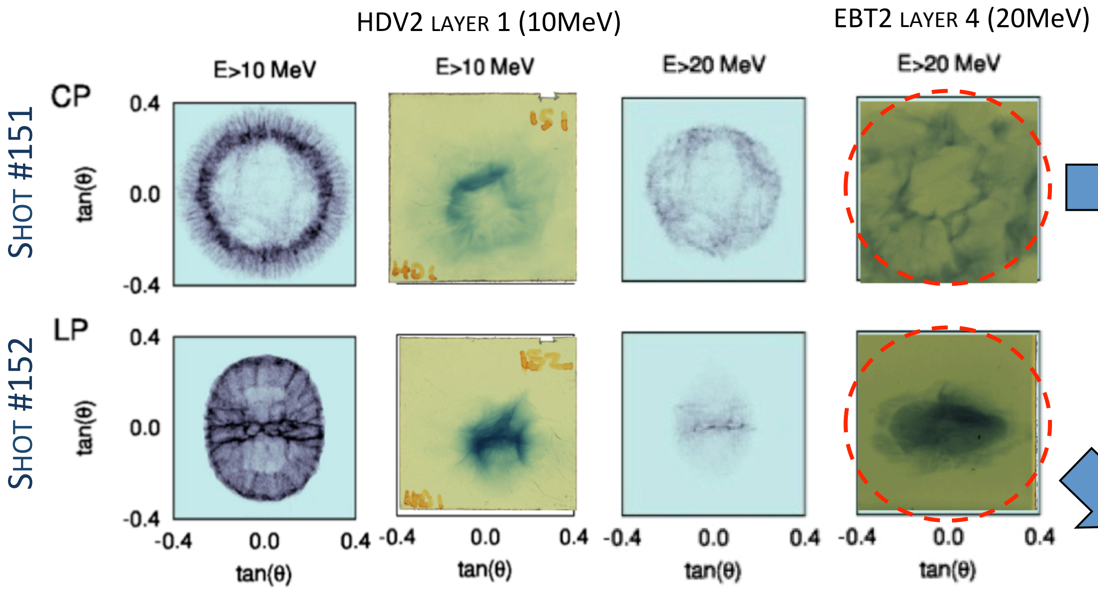

STRUCTURED, LARGER DIVERGENCE BEAM – UNSTABILIZED RADIATION PRESSURE DRIVE ?

RALEYGH-TAYLOR INSTABILITY

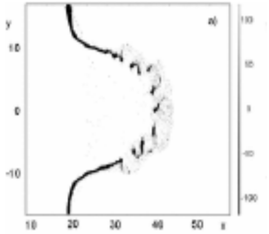

F.Pegoraro and S.V. Bulanov, PRL, **99**, 065002 (2007)

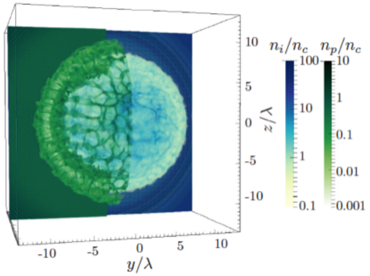

A.Sgattoni et al., PRE **91**, 013106 (2015)

ELONGATION IN POLARIZATION DIRECTION – SIGNATURE OF TRANSPARENCY ?

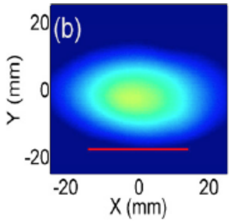

R. Gray et al, NJP, **16**, 093027 (2014)

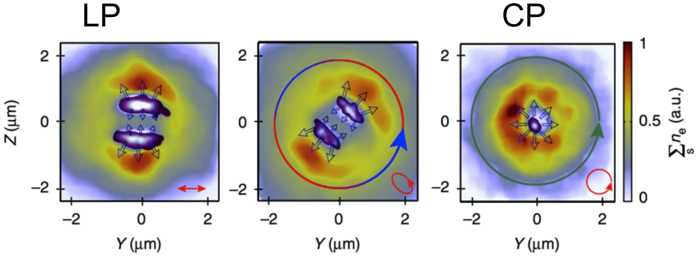

B. Gonzalez-Izquierdo *et al* Nat. Com. **7**:12891 (2016)

CARBON ION PROFILE USING CR39

CIRCULAR

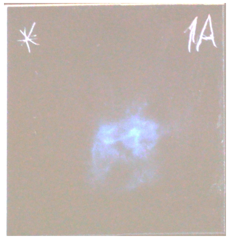

LINEAR

Radiation Pressure Acceleration at ELI-NP

T.Esirkepov, et al. PRL., **92**, 175003 (2004)

$$I = 1.37 \times 10^{23}\ \mathrm{W/cm^2}$$

$$\lambda \simeq 1\ \mu\mathrm{m}$$

$$n_e = 5.5 \times 10^{22}\ \mathrm{cm^{-3}}$$

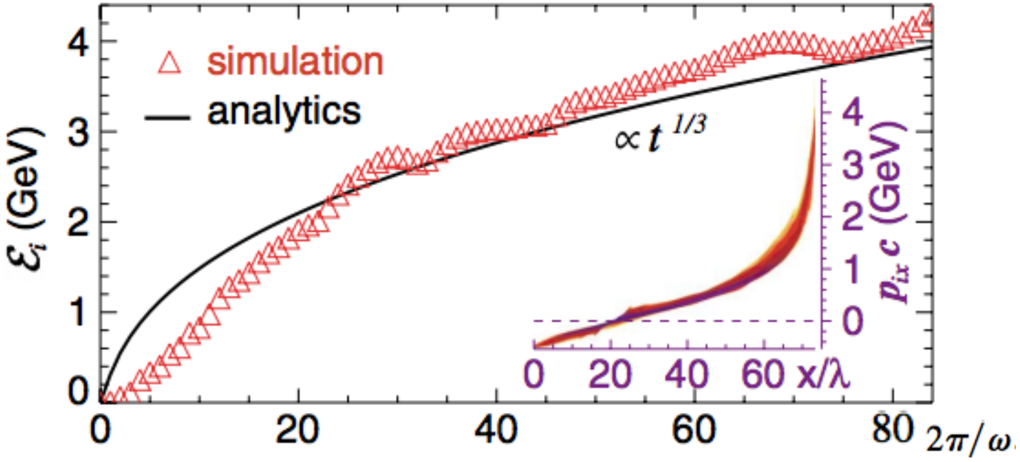

FIG. 2 (color). The maximum ion kinetic energy versus time and the ion phase space projection (x, p_x) at $t = 80 \times 2\pi/\omega$.

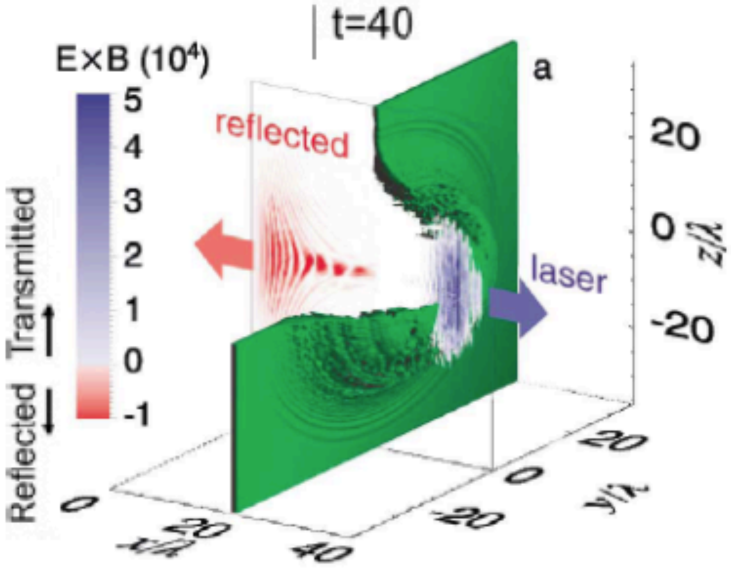

The ion density isosurface for $n = 8n_{cr}$

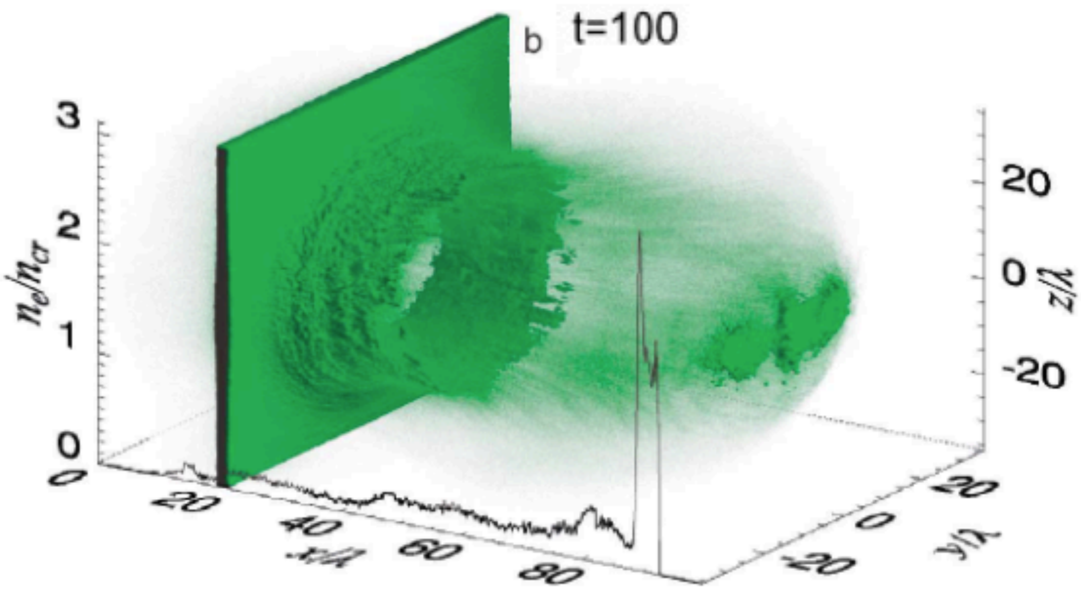

The isosurface for $n = 2n_{cr}$

Radiation Pressure Acceleration at ELI-NP

Near-100 MeV protons via a laser-driven transparency-enhanced hybrid acceleration scheme

A. Higginson et al, Nature Communications 9, 724 (2018)

$I_L = (3 \pm 2) \times 10^{20}\ \mathrm{W\,cm^{-2}}$ (PM contrast)

$\tau_L = (0.9 \pm 0.1)\ \mathrm{ps}$ (FWHM)

ℓ, in the range 10 nm–1.5 μm

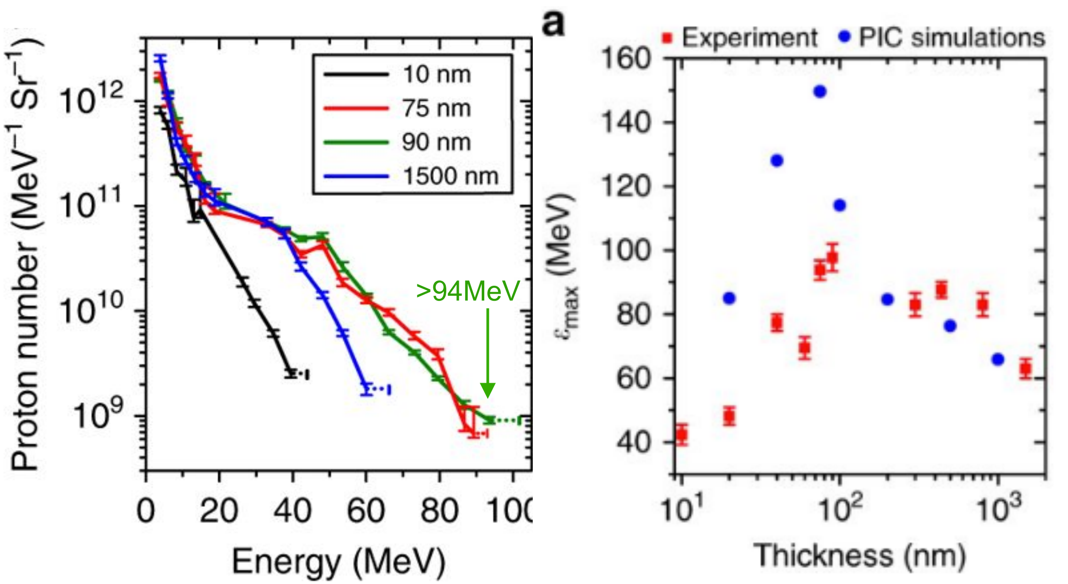

Main Laser

$(0.5\text{–}2.0) \times 10^{19}\ \mathrm{W\,cm^{-2}}$

Per-pulse @ -0.6ps

$(40\ \mathrm{fs};\ 1 \times 10^{22}\ \mathrm{W\,cm^{-2}})$

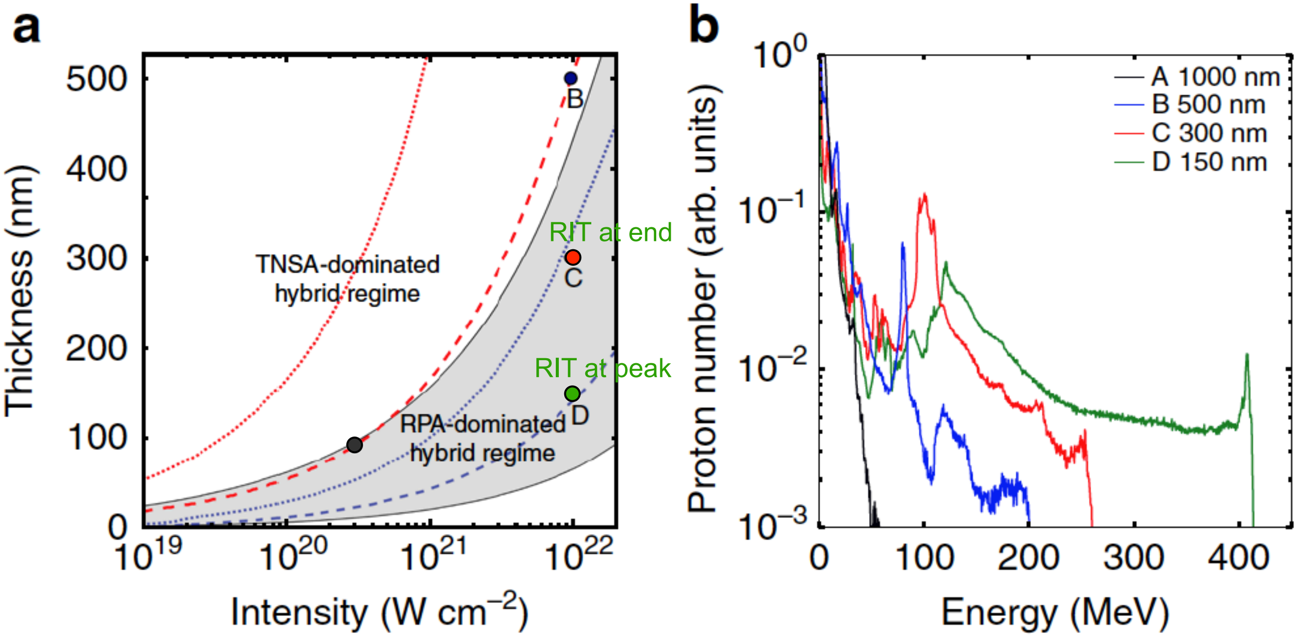

Enhancement of proton energy >2 for RIT

Radiation Pressure Acceleration at ELI-NP

Radiation dumping effects on ion acceleration at ultrahigh intensities ~ 10^{23}W/cm^2)

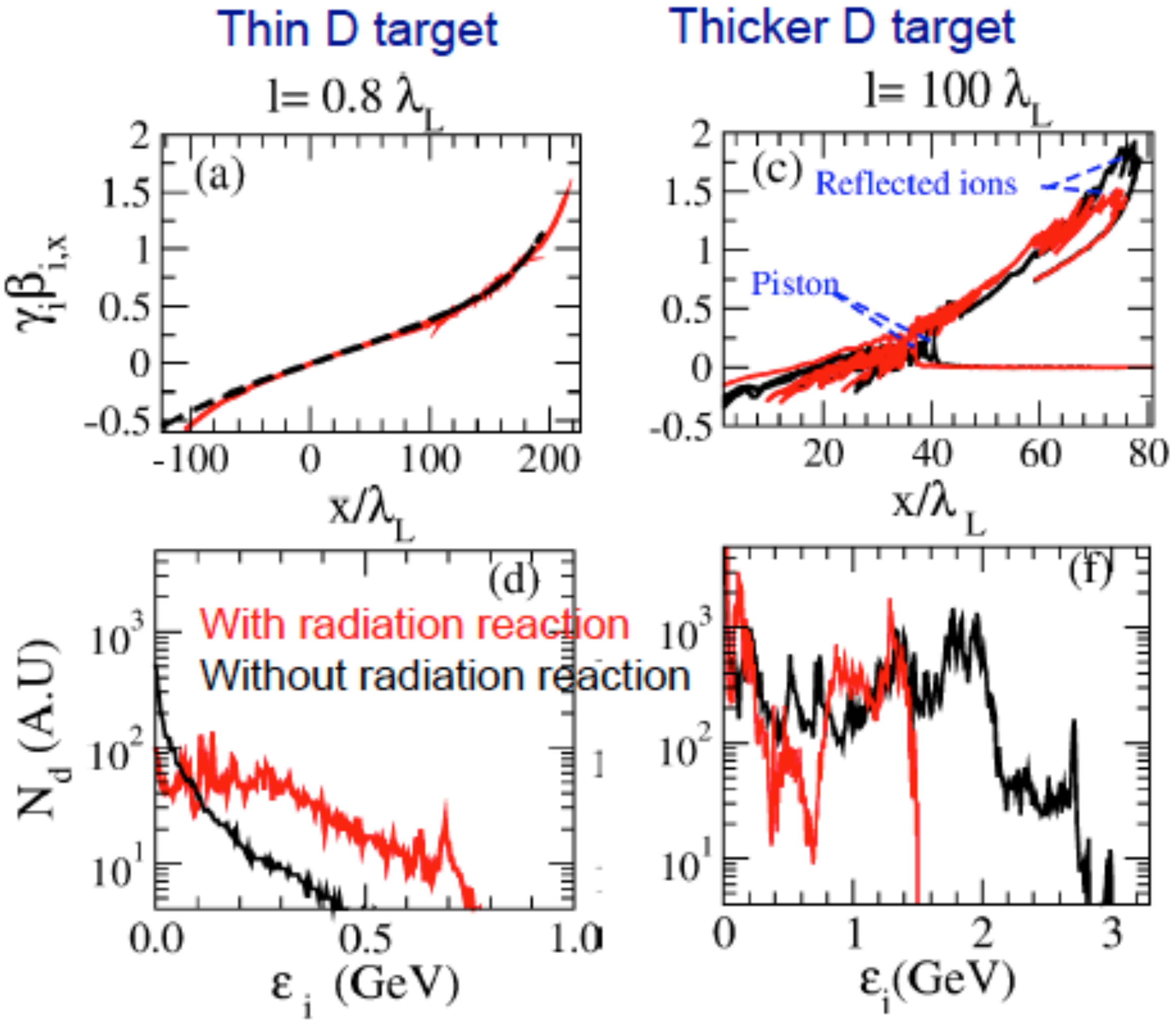

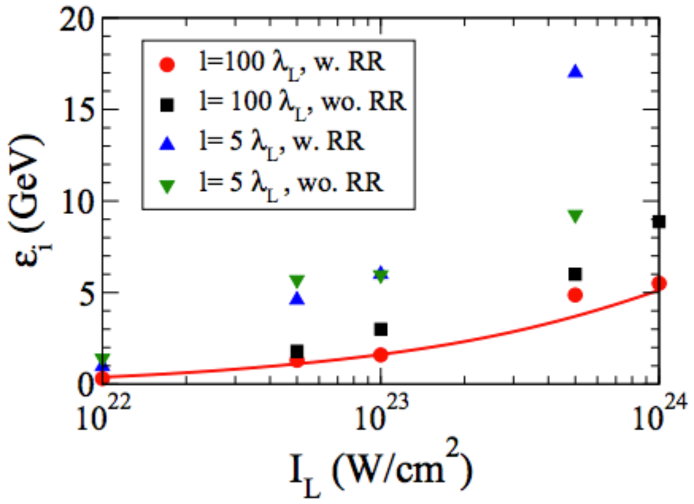

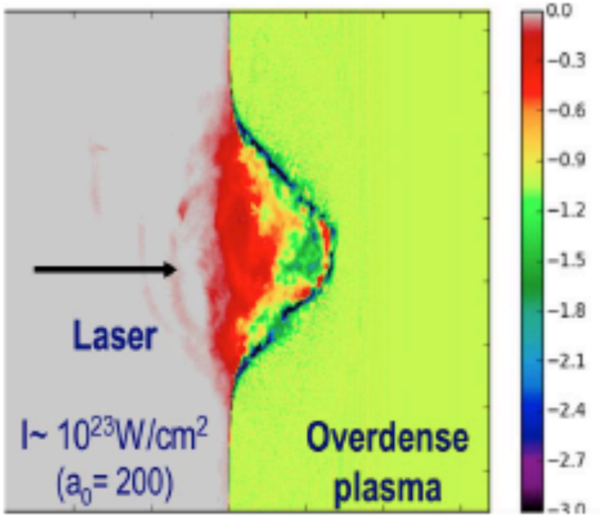

R. Capdessus & P. McKenna, Phys. Rev. E., 91, 053105 (2015)

Radiation Pressure Acceleration at ELI-NP

Efficient ion acceleration and dense electron–positron plasma creation in ultra-high intensity laser-solid interactions

D. Del Sorbo, New J. Phys. 20 (2018) 033014

5×10^{23} W/cm^2 < I_L < 1×10^{25} W/cm^2

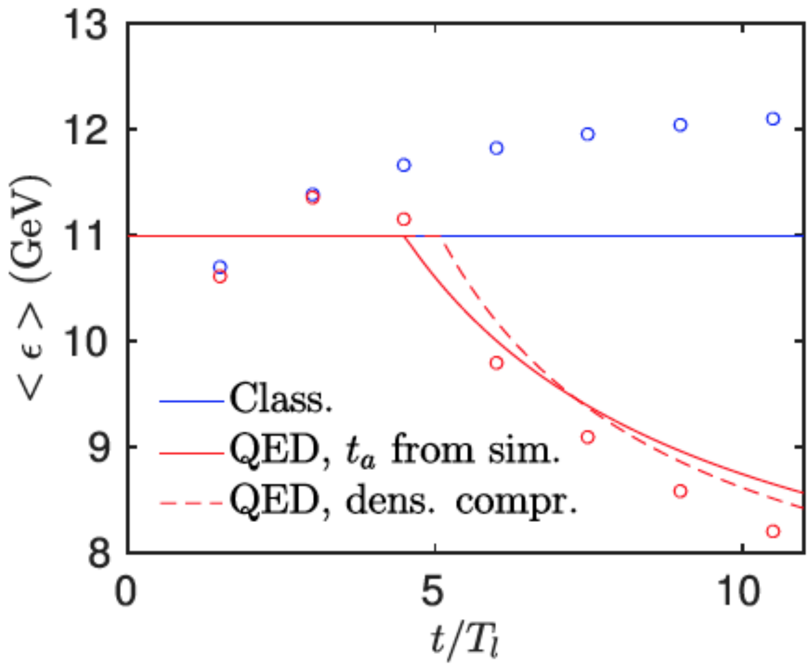

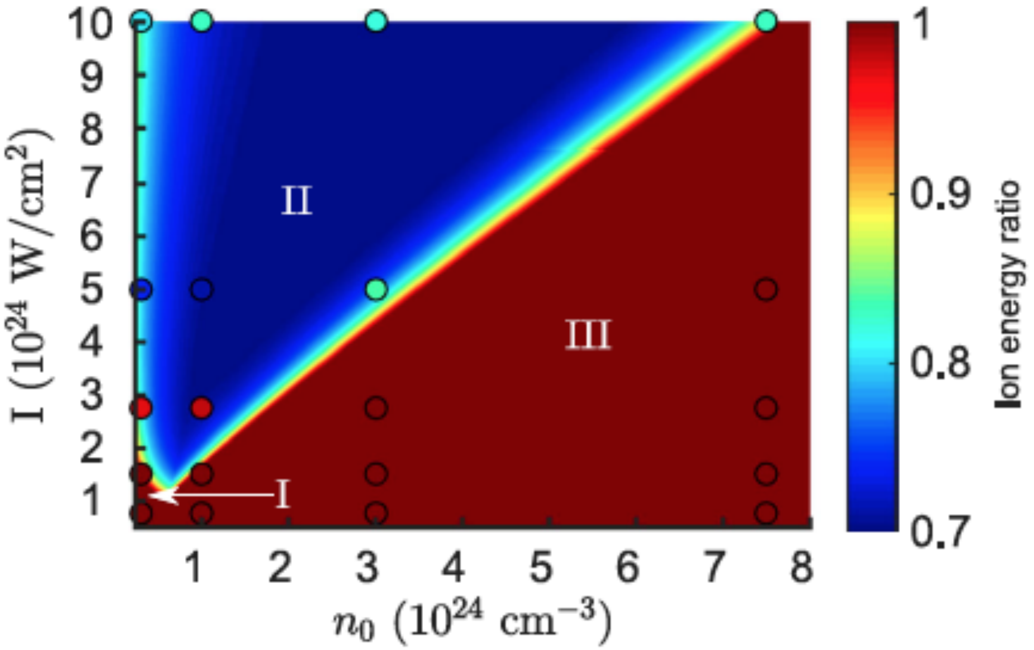

For a standard solid target ion start loosing energy for laser intensities above 10^{24} W/cm^2.

RPA scaling and conceivable max energies

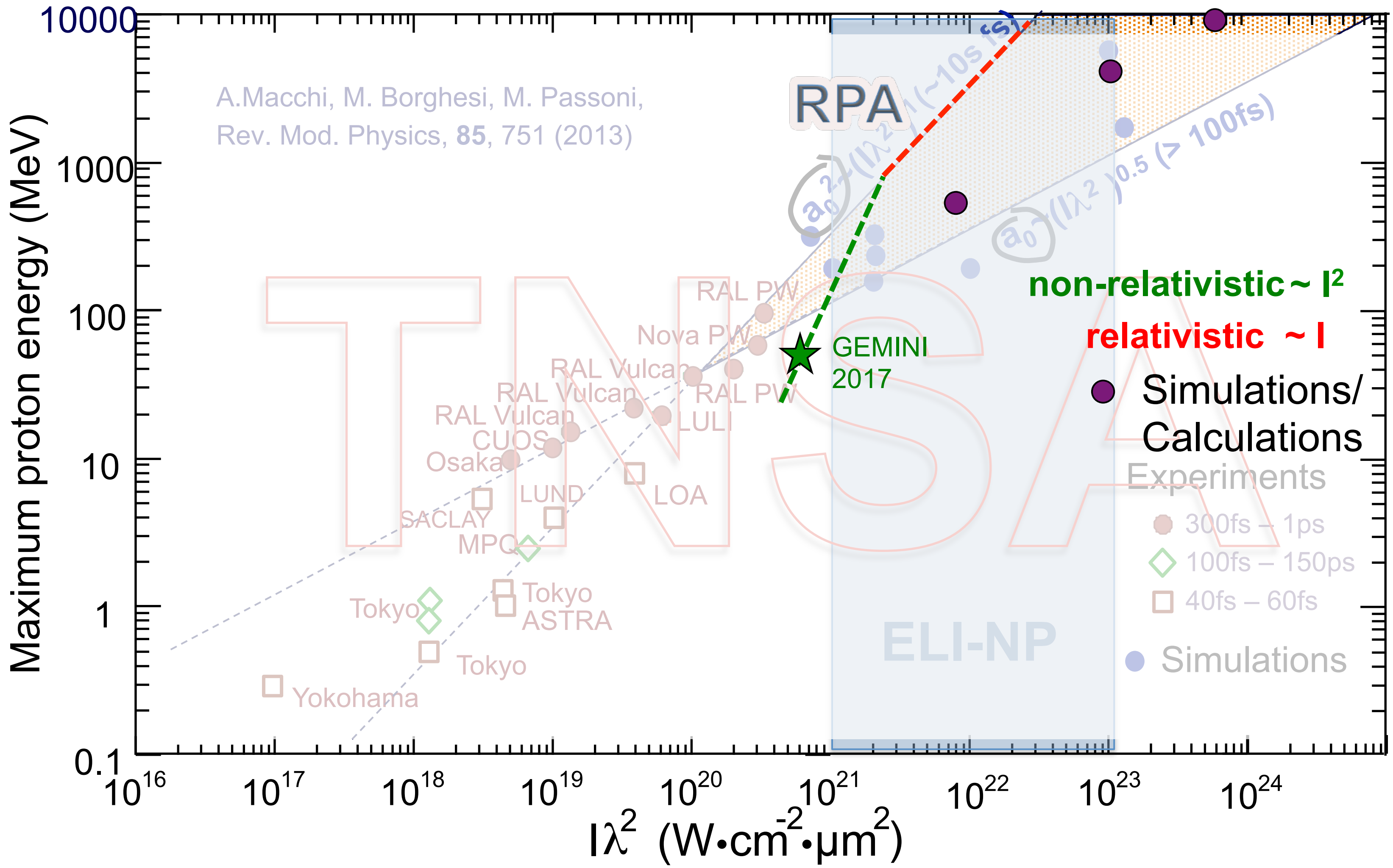

A.Macchi, M. Borghesi, M. Passoni,
Rev. Mod. Physics, **85**, 751 (2013)

EUROPEAN UNION

GUVERNUL ROMÂNIEI

Structural Instruments
2014-2020

Project co-financed by the European Regional Development Fund through the Competitiveness Operational Programme
"Investing in Sustainable Development"

Extreme Light Infrastructure-Nuclear Physics

eli
nuclear physics

(ELI-NP) – Phase II

IFIN-HH

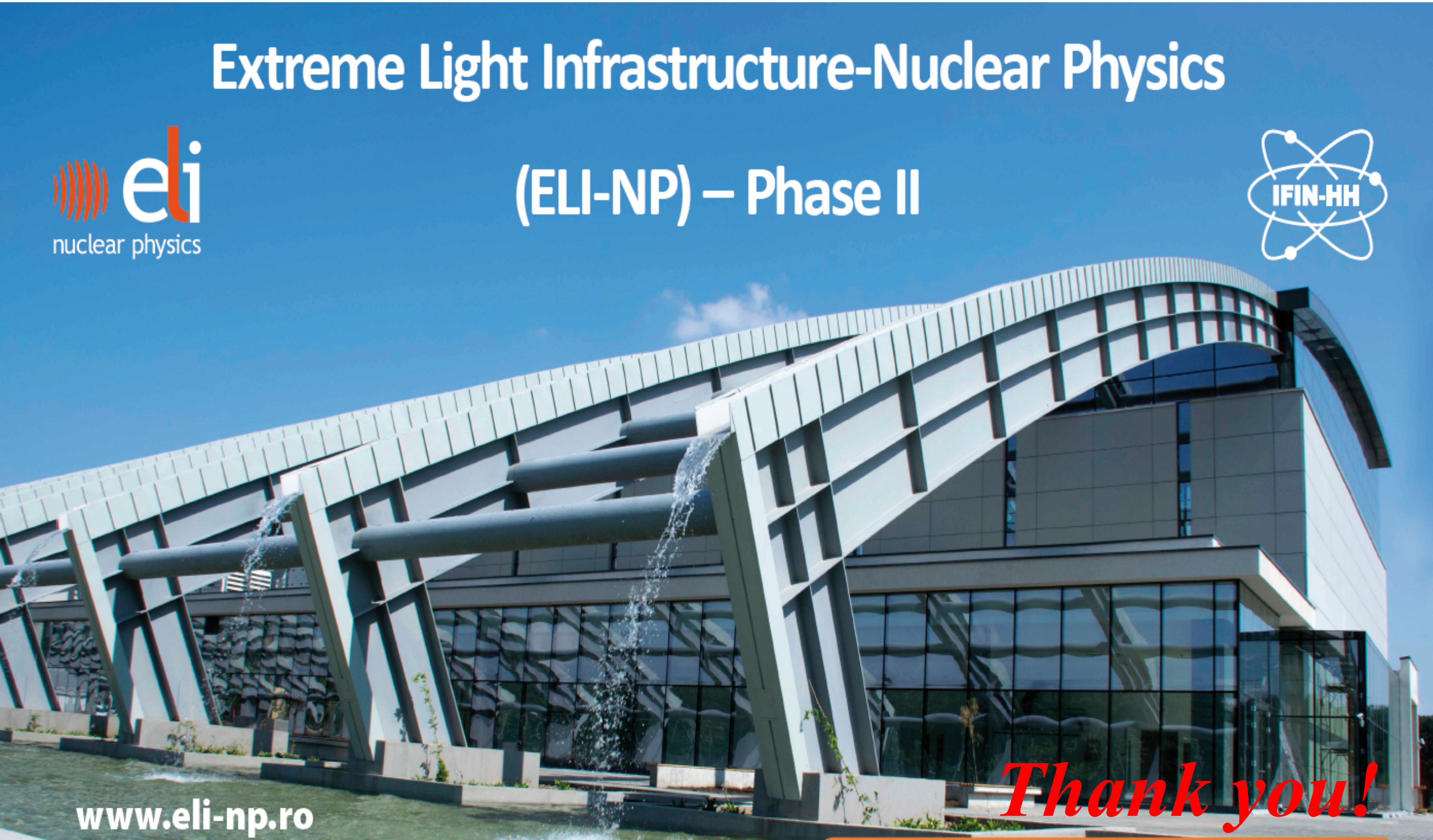

Thank you!

www.eli-np.ro